CANADA

PILLAR LOADING

PART I: Literature Survey and New Hypothesis

D. F. COATES

FUELS AND MINING PRACTICE DIVISION

DEPARTMENT OF MINES AND TECHNICAL SURVEYS, OTTAWA

MINES BRANCH

RESEARCH REPORT

R 168

Price $1.25

OCTOBER 1965

Available by mail from the Queen's Printer, Ottawa,
and at the following Canadian Government bookshops:

OTTAWA
Daly Building, Corner Mackenzie and Rideau

TORONTO
Mackenzie Building, 36 Adelaide St. East

MONTREAL
Aeterna-Vie Building, 1182 St. Catherine St. West

or through your bookseller

A deposit copy of this publication is also available
for reference in public libraries across Canada

Price $1.25 Catalogue No. M38 -1/168

Price subject to change without notice

ROGER DUHAMEL, F.R.S.C.
Queen's Printer and Controller of Stationery
Ottawa, Canada
1965

FOREWORD

It is Mines Branch policy to promote research, support universities and to disseminate information on subjects of importance to the mineral industry. With the traditional strength, among other subjects, of McGill University in applied mechanics, it has been natural for its Department of Mining Engineering and Applied Geophysics to display a leading interest in the development of the new subject of rock mechanics and in the training of post-graduate students in this subject. The cooperative effort of our two organizations has produced in a doctoral thesis, on which this report is based, what seems to be a significant contribution to the science of mining.

Dean D. L. Mordell and Professor R. G. K. Morrison, Chairman of the Department of Mining Engineering and Applied Geophysics, are to be commended for promoting this work. Mines Branch is glad to publish this work so that it can receive wide distribution amongst those interested in a basic study of an important element of mine structures -- the pillar.

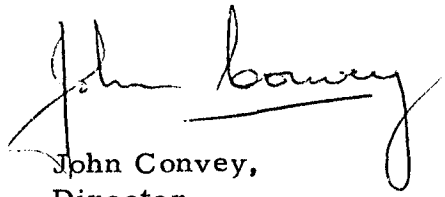

John Convey,
Director,
Mines Branch.

Mines Branch Research Report R 168

PILLAR LOADING. Part I: Literature Survey and New Hypothesis

by

D.F. Coates[x]

- - -

ABSTRACT

This research work on pillar loading is in what might be described as the area of engineering theory. As such, it is concerned largely with the combining of existing scientific theories into a rational hypothesis for predicting the loading of pillars. Hitherto, this has been possible only in a very crude way and only for horizontal workings using the tributary area theory.

In previous work on this subject, some workers have recognized that rock is not a fluid material applying a dead weight to pillars but, rather there will be a structural reaction of the wall rock on the excavation of the vein rock. However, no complete analysis of the mechanics of the system in producing pillar loading had been established.

The first step in this research work, therefore, has been to analyse the structural aspects of the problem by solving the statically indeterminate net deflection of the walls. This net deflection at the pillars will be a measure of the increase in pillar stress resulting from mining. The resulting equations show that not only is the extraction ratio important in determining pillar loading but that the hitherto ignored parameters of the ratio of field stress components normal and transverse to the mining zone, the height of the pillar, the location of the pillar within the mining zone, the ratio of compressibility of pillar rock to wall rock, the number of pillars across a typical section of the mining zone, the breadth of the pillar, and the ratio of the depth from the ground surface to the span of the mining zone are all of some significance.

---

[x]Head, Mining Research Laboratories, Fuels and Mining Practice Division, Mines Branch, Department of Mines and Technical Surveys, Ottawa, Canada.

Additional analytical work has been done in examining the various alternatives to the hypothesis that is based on elastic ground. In this work it is shown that for compatible strain the loading of pillars will almost always be a phenomenon associated with elastic, or at least pre-failure, deformation in the walls. Consequently, any mechanisms based on post-failure rock properties will not be applicable to this problem, although they may be for other types of support. In this supplementary work, an elliptical arching theory has been developed that may be more valid than the various other theories hitherto available for this case of loading of yielding support.

Direction des mines

Rapport de recherches R 168

LA CHARGE DES PILIERS. PARTIE I: DOCUMENTATION ET NOUVELLE HYPOTHÈSE

par

D. F. Coates*

RÉSUMÉ

Le présent travail de recherche sur la charge des piliers se range dans ce que l'on pourrait appeler le domaine du génie théorique. Essentiellement, il cherche à combiner les théories scientifiques existantes pour en arriver à une hypothèse rationnelle sur la prédiction de la charge des piliers. Jusqu'ici, cela n'a été possible que d'une façon très rudimentaire et seulement dans le cas où l'extraction se faisait à l'horizontale en utilisant la théorie de la zone tributaire.

Dans des travaux précédents sur le sujet, quelques chercheurs ont reconnu que la roche n'est pas une matière fluide qui applique un poids mort aux piliers, mais qu'il se produit une réaction structurale de la roche encaissante lors de l'extraction de la roche du filon. Cependant, on n'a pas fait d'analyse complète de la mécanique du système à mesure que l'on charge les piliers.

Par conséquent, la première étape dans le travail de recherche a été d'analyser les aspects structuraux du problème en déterminant statiquement la déflexion nette des parois. Cette déflexion nette aux piliers servira à mesurer l'augmentation de la charge que supportent les piliers à la suite de l'extraction. Les équations qui en résultent indiquent que non seulement le taux d'extraction est important pour calculer la charge des piliers, mais que les paramètres naguère inconnus du rapport des composantes des contraintes de terrain normales et transversales à la zone d'extraction, la hauteur du pilier, l'emplacement du pilier dans la zone d'extraction, le rapport de compressibilité de la roche du pilier à la roche encaissante, le nombre de piliers à travers une coupe typique de la zone en exploitation, la largeur du pilier et le rapport entre la profondeur et l'étendue de la zone en exploitation ont une certaine importance.

*Chef, Laboratoires de recherches sur les mines, Division des combustibles et du génie minier, ministère des Mines et des Relevés techniques, Ottawa, Canada.

L'auteur s'est livré à un travail analytique supplémentaire en soumettant à diverses conditions cette hypothèse qui est fondée sur l'élasticité du terrain. Il en ressort que pour une fatigue compatible, la charge des piliers sera presque toujours associée à une déformation élastique ou, du moins, une déformation précédant la rupture de la roche encaissante. En conséquence, nul mécanisme fondé sur les propriétés de la roche après la rupture ne peut s'appliquer à ce problème, bien qu'on puisse utiliser de tels mécanismes pour d'autres genres de support. Dans ce travail supplémentaire, une théorie de cintre elliptique a été mise au point qui pourrait être plus valable que toutes les autres connues jusqu'à aujourd'hui au sujet du chargement du support fléchissant.

CONTENTS

	Page
Foreword	i
Abstract	ii
Résumé	iv
Statement of the Problem	1
Literature Survey of Previous Work	4
Method of Approach	20
Hypothesis of Pillar Loading	22
Long, Deep Mining Zone	22
Introduction	22
Tributary Area Theory	23
Deflection of a Circular Hole due to Applied Uniaxial Plane Stress	25
Deflection of a Circular Hole due to Excavation in Uniaxial, Plane Stress	25
Deflection of a Circular Hole due to an Internal Uniaxial Traction	26
Deflection of a Circular Hole due to Applied Biaxial, Plane Stress	27
Deflection of a Circular Hole due to Excavation in Biaxial, Plane Stress	28
Deflection Around an Elliptical Hole at $x' = 0$ due to Excavation in Hydrostatic Stress, Plane Strain with $\mu = 0.5$	29
Deflection of an Elliptical Hole at $x' = 0$ due to Applied Uniaxial Stress, Plane Strain	30
Comparison with Two Special Solutions	32
Pillar Load and Average Stress from Deflections	34
Reverse Deflection of Wall due to Average Pillar Pressure	38
Distribution of Pillar Loads	38
Local Penetration of Pillars into the Walls	41
Pillar Formula Resulting from Deflection Hypothesis	43

CONTENTS (Cont'd)

	Page
Long, Shallow Mining Zone	44
Introduction	44
Deflection of a Restrained Beam	44
Reverse Deflection of Roof due to Average Pillar Pressure	51
Distribution of Pillar Loads	51
Pillar Formula for Shallow Workings	53
Comparison of Shallow Case with Deep Case	55
Alternatives to the Elastic Analysis	55
Yielding Wall Rock with Horizontal Workings	55
Arching from Bending over Horizontal Workings	61
Elliptical Arching	68
Acknowledgements	70
Bibliography	71
APPENDIX - Glossary and Abbreviations	78

- - -

FIGURES

No.		Page
1.	Variation of Pillar Load with Pillar Stiffness (Ref. 8)	5
2.	Deflection of a Circular Hole	25
3.	Stress Concentration from Internal Uniaxial Traction in a Circular Hole	26
4.	Deflection of a Circular Hole in Biaxial Plane Stress	27
5.	Geometrical Relations in a Circular Hole	28
6.	An Elliptical Hole in a Biaxial Stress Field	29
7.	Deflection of a Slit in a Uniaxial Stress Field	33
8.	Deflection of a Pillar	35
9.	Approximation for Abutment Compression	37
10.	Deflection Curves With and Without Abutment Compression	37
11.	Circular Inclusion in a Uniaxial Stress Field	38
12.	Deflection of the Edge of a Semi-Infinite Plate	41
13.	A Long, Shallow Mining Zone	45
14.	Coordinates for Deflection Calculation	47
15.	Free Body Diagram of Roof Rock	48
16.	Deflection of Beam with Elastic Supports	49
17.	Variation of K_b' with z'	54
18.	Comparison of Pillar Loading Theories	56
19.	Stresses in Yielding Ground Over an Opening	58
20.	Mohr Circle of Stress for Abutment Zones	59
21.	Variation of Average Pillar Pressure with Span of Mining Zone	59
22.	Arching-Bending Over Horizontal Workings	62
23.	Bending Moment Diagrams for Arching-Bending	63
24.	Doming Over Horizontal Workings	66
25.	Elliptical Hole in Biaxial Stress Field	68
26.	Elliptical Arching Over Horizontal Workings	69

- - -

STATEMENT OF THE PROBLEM

As related to mining, pillars can be defined as the in situ rock between two or more underground openings. The terms height, thickness and width should be restricted to the dimension normal to the plane of the workings or openings. The length of the pillar is the greatest dimension in this plane, and the breadth can be used for the lesser dimension in this plane (1)[x].

In examining the mechanics of pillars there are two aspects to be considered. First, the load that is applied to the pillar must be determined. Then, secondly, the strength of the pillar, taking into account the various modes of failure, should be appraised. The safety factor can then be determined and judgment exercised on whether it is adequate or not.

Throughout the various fields of structural mechanics, experience has shown that design can be based either on detailed theoretical stress analysis, with elaborate and refined testing techniques on the material (i.e., taking into account stress concentrations, repetitions of loading, and some non-linear aspects of the materials), or on analogue testing together with a simple, somewhat superficial, analysis of stress.

In rock mechanics for designing pillars the use of the first alternative would require, among other things, proof that theoretical, elastic stress concentrations actually occur in the rock. For this proof a large amount of basic field work, using measuring techniques that are not yet fully developed, would be necessary. Considering the rheological and structural nature of rock, it is probable that the theoretically calculated stress concentrations in many, or possibly in most, cases do not actually occur. The often observed evidence of surface relaxation and incipient slabbing in the zone where the maximum tangential stress should be occurring supports this view. Also, some field measurements indicate that the theoretical stress concentrations are not obtained (2) and that a plastic-type stress distribution often occurs (3).

The first design alternative, of ideal stress analysis and testing, would also require the perfection of current testing techniques to obtain absolute strength values, which we are far from obtaining as the first requirement of producing homogeneous compressive stresses in

---

[x] These numbers refer to the sources of information listed in the BIBLIOGRAPHY at the end of this report.

laboratory specimens has not yet been achieved. It also would require knowledge of how to relate this absolute strength of the rock substance to that of the rock mass. Some evidence exists that rock masses may only have strengths equal to about 2% of the nominal (from conventional laboratory tests) strength of the rock substance (4), and the cases that have been analysed by the author indicate that it might be less than 1%. Moreover, these comparisons are for situations where no gross structural weaknesses were known to exist to cause obvious reductions in the strength of the rock masses.

Finally, with respect to the first alternative it can be said that this procedure has not been followed in developing the subjects of structural engineering or soil mechanics, which possibly have enough similarity to rock mechanics for this experience to have some pertinence. The procedure in structural mechanics over the past 100 years and in soil mechanics over the past 40 years has been to gradually replace decisions based on pure judgment with those guided by mathematical analyses. These analyses have generally been in terms of simple theories of stress distribution (ignoring such factors as stress concentrations) together with, in effect, relatively crude analogue testing supported and modified by experience and research.

In the case of pillars, the second design alternative, that followed in the above related subjects, would be based on the determination of the total load rather than on the detailed stress distribution. Certainly total load is a more significant parameter for the total energy content of the pillar; or, alternatively, average stress is more significant for the average energy content per cubic foot of ground than is the maximum stress concentration which exists over a small part of the rock surface and for an infinitesimal depth. Consequently, it is possible that total load, or average stress, is a more significant parameter for rockburst-type failures.

Furthermore, for typical mining openings of rectangular cross-sections the stress concentrations in the pillars occur near the walls (i.e., hangingwall and footwall) where failure is least likely. On the other hand, near the central part of the pillar, where failure is most probable, the variation of longitudinal stress (i.e., normal to the walls) across the pillar is slight (60). It has been observed that at this central section the confinement resulting from the restraint of the walls is at a minimum and hence the central section is potentially less stable than the section near the walls (60).

Also, intuitively one feels that weight or total load is more significant in producing instability than is a local stress concentration. For example, the stress concentration in an infinitesimal depth of ground at a sharp corner might be theoretically as much as 10, which might produce

a tangential stress of 20,000 psi; however, this stress would be much less significant than an average stress in the pillar of 20,000 psi or 10,000 psi, or possibly even 5,000 psi. Furthermore, two cases could be obtained where the maximum stresses from stress concentrations might be equal, but in the first case the average pillar stress could be twice the average pillar stress in the second case. Other things being equal, there would be no doubt that the first pillar would not be as safe as the second.

Another aspect of the importance of load is that the deflection or compression of a pillar should be a function of load or average stress to a larger extent than of stress concentrations near the surface. This total deflection should be closely related to the stability of the pillar; consequently, stability is a function of load. However, our knowledge of how pillars actually fail is still sufficiently sparse that these statements cannot be made with certainty.

In using the second design alternative there is an advantage in that the simple uniaxial compression test provides a good analogue of normal pillars. In other words, the restraint that the walls provide at the ends of the pillars is reproduced by the restraint of the platens on the ends of the laboratory specimens. For this reason the specimens can have a stress distribution similar to the stress distribution in pillars.

It is also conceivable that, by testing a series of specimens to determine the effect of size on average strength, a relationship could be obtained that could be extrapolated to the size of the actual pillars. To provide some support for such a long extrapolation, studies have shown that there can be a strong similarity between the microscopic or petrofabric pattern of cracks and those of the macroscopic or joint patterns of the rock mass (5), and such a connection with respect to strength has been indicated empirically (4).

From the above reasoning it follows that one problem that must be solved in the field of rock mechanics in connection with pillars is the analysis of pillar loads. This is the problem to which this research work contributes. A review of existing knowledge on the subject provides a starting point.

LITERATURE SURVEY OF PREVIOUS WORK

The main contribution to the analysis of pillar loads was made some time ago (6). By assuming that the entire weight of the ground overlying the tributary area in horizontal workings is supported by the pillar, a simple equation was obtained: $\sigma_p = S_o/(1-R)$, where σ_p is the average pillar stress, S_o is the vertical field stress acting at the level of the mining zone, and R is the extraction ratio in the mining area (the area mined divided by the total area). It follows from this equation that for 50% recovery the average pillar stress would be twice the original stress in the pillars, S_o, before mining; for 75% recovery, the average pillar stress would be $4S_o$; and as 100% recovery is approached, the average pillar stress would approach infinity.

This simple concept, which is labelled here the "tributary area theory", ignores, among other factors, the effect of the resistance to deformation of the roof or overlying ground. At the same time, even ignoring the possibilities of differential pillar loading due to geological structural features, this equation, as will be shown later, does not provide an upper limit for the average pillar stress. Nevertheless, a recent review of the subject showed that no other analytical expression was available for the calculation of pillar loads (7).

Shortly after the establishment of this theory, some experiments showed the importance to pillar loading of the deformation properties of the ground (8). Photoelastic models were used to determine the stress distribution around rooms and pillars and to show how this stress distribution changed with the stiffness of the pillar. It was demonstrated that with a pillar of lower stiffness than the model material (see Figure 1) most of the field stress was deflected around the two rooms and pillar into the outside abutments. However, no analysis of the data was made to provide a quantitative method for the determination of the obviously reduced loads, or stresses, in the pillars.

Some intuitive rules have been formulated that, in effect, take into account to some extent the deflection aspect of the problem (9). It was postulated that the maximum pillar load would occur when the radius of the stoping area was equal to the depth of the mining zone divided by the extraction ratio. (The definition of extraction ratio in this reference is equal to the total area of the mining zone divided by the area of the pillars.) It was further stated that the maximum pillar load would be found at the centre of the mining zone and would be equal to the overburden load of the tributary area. The average stress for the other pillars would decrease towards the abutments becoming equal to the overburden stress at the

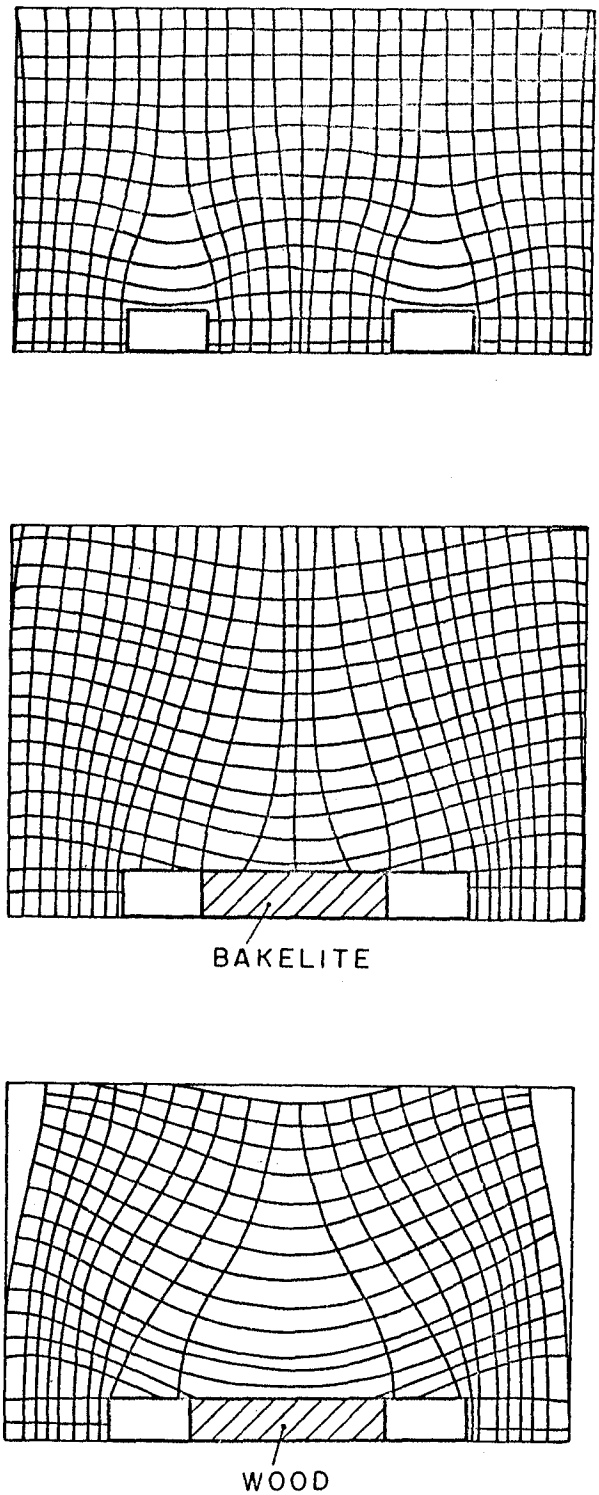

Figure 1. Variation of Pillar Load with Pillar Stiffness (Ref. 8)

abutments, which, of course, ignored the stress concentrations in the abutments. Neither theoretical analyses nor measurements were given to justify these statements.

In a paper based on the results of photoelastic experiments on the stress distribution in pillars, it was stated that when the breadth of the mining zone, L, was equal to the depth below the surface, z, the central pillars in the mining zone would carry the full overburden load of the tributary area (10). Unfortunately, no experimental results were presented.

An attempt has been made by other workers to explain the collapse of roofs in mines that are being worked by the room and pillar method (11). The theory that was formulated took into account the weight of the overburden, the bearing reactions of the abutment, and the reactions of the pillars. However, the emphasis in this work was on calculating bending stresses in the overlying ground rather than on determining pillar loads and predicting their stability, and no general theory was provided. This type of analysis does not take into account, among other factors, the contribution to closure of the deflection of the floor.

The initial work of the author in this field took into account, to some extent, the stress distribution created by mining in a horizontal seam (12). Recognition was given to the transfer of load through shear stresses into the abutments. The effect of excavating the rooms or stopes was postulated as being equivalent to applying at the roof level a vertical stress acting downwards equal to the vertical stress that had been acting upwards from the excavated ground on the roof.

The effect of this additional vertical stress acting downwards at the depth of the workings and over the finite area of the workings must produce a deflection downwards of the overlying ground. If the overlying ground extended vertically to infinity, the deflection of any point in the overlying ground could be calculated following the integration over the roof/pillar interface of Boussinesq's equation for the stress distribution resulting from a point load acting on the surface of a semi-infinite solid. It was then reasoned that, because the overlying ground did not extend to infinity but had a free surface at the ground level, the deflection at the ground level resulting from the additional downward stress applied at the level of the workings would be twice the deflection that would exist at the ground surface elevation if the overburden did extend to infinity.

This work was the first analysis to show quantitatively that when the ratio of the span of the workings, L, to the depth of the workings, z, is low the average pillar stress in the central pillar should be less than the overburden load arising from the area tributary to the pillar (12). For example, it was shown that when $L/z = 0.5$ the central pillar would have an average stress equal to, for an extraction ratio of 75%, 2.5, rather than 4,

times the original field stress, which would be about 60% of the overburden load of the tributary area.

There were several limitations in this theory. The principal deficiencies were that the average pillar stress could only be calculated for the central pillar and that the integration of the equivalent stress caused by excavation had to be done using a graphical method rather than having the convenience of an analytical expression (12). It did, however, provide a general basis for departing from the simple theory that was available up to that time.

This work also provided an analysis of pillar loads in horizontal workings when the overburden yielded under the shear stresses produced by stoping (12). The stress distribution in the overburden and the loads in the pillars in this case are dependent on the shear resistance of the ground as well as on L/z[x]. As the deflection of the roof does not enter into this analysis, the calculated average pillar stresses are all equal. Actually there would be a variation from a maximum at the centreline to a minimum at the abutments similar to the elastic case.

In a review of room and pillar mining in eastern Europe, the effects of using barrier pillars was discussed by one research worker (14). It was claimed that at a certain magnitude of L/z and a suitable width of the barrier pillars, deformation produced a natural vault above the rooms and intervening pillars. In other words, it was postulated that arching occurred between the barrier pillars which thus sustained some of the load that would otherwise have to be taken by the normal pillars. Consequently, these normal pillars could be reduced in size and the extraction ratio of the area between the barrier pillars increased. It was also pointed out that the reduction in stress would be greatest on the pillars adjacent to the barrier pillars and be less pronounced in the centre of the mining zone. This paper definitely indicated an awareness of the effects of L/z but not of the other factors that can be significant.

Over the years the investigation of the stability of workings in potash and salt had led some investigators to the observation that when a certain size of mining zone was exceeded, the hangingwall would bend so that pillars that seemed to be quite stable and apparently oversize during the initial operations would be destroyed (13). This was a useful qualitative deduction.

---

[x] Symbols are defined when they first appear in the text; in subsequent sections the reader can obtain the definition by consulting the Appendix.

In attempting to establish a rational design procedure for mining horizontal beds of potash, it was assumed by one worker that the overlying ground would behave like a clamped plate up until the tensile strength of the roof rock was exceeded (15). Using the tensile strength obtained on laboratory samples, calculations were then made to determine the span that would produce these tensile stresses by pure-bending. The concept being used was that when the tensile stresses were exceeded the strain energy in the overlying roof rock would then be released, producing the rockbursts that were observed from time to time. It was mentioned that the properties of the rock mass would be different than those of a sample; however, no recognition was given to the difficulty of testing for tensile strength, nor to the questionable procedure of attributing any tensile strength to a rock mass.

Following previous mathematical work (11), the effects on pillar loads of the deflection characteristics of the overlying ground in horizontal workings were calculated (16); however, the significant factors, such as floor deflection, omitted in the previous work were also omitted in this analytical work. It was claimed that the relative effects were qualitatively substantiated by observations in potash mines. However, no measurements were presented in the paper. One concept introduced, but not proven, looks interesting; it is that the modulus of deformation of a pillar varies with its breadth. It is conceivable that some such relation might exist, and if substantiated important deductions could be made.

Several laboratory photoelastic studies have been made on the distribution of stress in pillars (6, 8, 10, 14, 17, 18, 19), which both confirmed the theoretical stress distributions for multiple circular openings (20, 21, 22) and added additional information on geometries not covered by theory. However, few measurements underground have been made to appraise the theoretical or laboratory work; the little evidence that exists indicates the presence commonly of near-surface zones of reduced stress rather than of increased stress (23, 24, 25, 26).

In some of this photoelastic work the results were analysed to give pillar loadings as well as the stress distribution (17, 19). The results of these experiments showed clearly that the pillar loadings were invariably less than prediced by the tributary area theory. No explanations were offered for this finding.

Other experiments where pillar loadings were measured involved the use of mortar models (17, 78). Again these experiments showed the measured loads to be less than predicted by the tributary area theory.

In addition to the above work, an extensive series of laboratory experiments was conducted on the stress distribution occurring in model pillars where the dip of the seam varied from 0^{o} to 90^{o} (27). The models were constructed of gelatin, and the stresses were determined by photoelasticity,

As a result of this work it was found that the average normal and tangential stresses could be calculated using simple approximations (27). For dips between 0^o and 30^o, it seems possible to obtain a close approximation to the average pillar stresses by assuming the dip as 0^o. For dip angles between 60^o and 90^o, the dip angle can be assumed to be 90^o. For dip angles between 30^o and 60^o, the average stresses can be then be determined by the equations based on a simple resolution of forces:

$$\sigma_p = \gamma z \, (\cos^2 i + k \sin^2 i) \, A_t/A_p$$

and

$$\tau = \tfrac{1}{2} \gamma z \sin 2i \, (1 - k) \, A_t/A_p,$$

where σ_p is the average normal stress, γ is the density of the overlying ground, z is the depth to the pillar, i is the dip angle, A_t is the area tributary to the pillar, A_p is the cross-sectional area of the pillar in the plane of the seam assuming that the sides of the pillar are normal to the walls, $k = S_h/S_v$ (i.e., horizontal to vertical field stress ratio), and τ is the average shear stress across the pillar. These model tests provide a basis for determining the effect of dip angle on pillar stresses; however, their design was not suitable for the obtaining of the actual magnitudes of pillar stresses.

Besides the above theoretical and laboratory work, some underground measurements have been made. One of the first attempts to measure pillar stress was done indirectly by measuring the velocity of sound through the pillar (28). Previous work in the laboratory indicated that the velocity varied with the magnitude of the stress in rock samples (29), although the variation of velocity with stress was rather small.

The phenomenon was used in one particular mine (28). By comparing the velocities obtained in the pillars with the velocities obtained on small samples of the rock from the pillars, it was found that the differences between the velocity readings obtained from any two pairs of holes in the pillars and the difference between these velocities and the average velocity obtained on the test specimens at zero stress were all, within the experimental error, equal. The results thus indicated that the pillars were not subjected to sufficient stress to be measurable by this technique. It was suggested that the load of the overlying ground was being transmitted by arch action into the abutments of the stopes. However, no attempt was made to analyse this action.

In this same work a test pillar was reduced by excavation to one-half of its original cross-sectional area (28). The velocity in it, and the adjacent pillars, showed no significant change, suggesting no change in stress from the initial test in the full size pillar.

The test pillar was then cut free from the roof, so that it could be guaranteed that the average stress in the pillar was substantially zero (28). The velocity through the pillar then fell from the previous value of 4755 metres per second to about 300 metres per second, whereas the velocity in the adjacent pillars remained approximately the same. The low velocities in the test pillar were attributed to the pillar's being shattered to such an extent that the acoustical path between the test holes was altered substantially, hence making it impossible to deduce stress magnitudes from a physical interpretation of the readings.

In another paper a brief description is given of some measurements of stress in the pillars of a potash mine (25). Two unidirectional electrical wire strain gauges were cemented at the end of a borehole at right angles to each other. The stress in the end of the borehole was then relieved by extending the hole with a coring bit. It was assumed that the change in strain resulting from this overcoring was a measure of the normal stress in the pillar at that point.

In pillars at a depth below the ground surface of 429 metres, one set of measurements produced, as an average of several readings, a vertical stress of 142 ksc and a horizontal stress of 102 ksc with a second set of readings producing a vertical stress of 96 ksc and a horizontal stress of 59 ksc (25). A third set of readings in a pillar at a depth of 498 metres produced a vertical stress of 96 ksc and a horizontal stress of 45 ksc.

Although the dimensions of the pillars and the mining zone were not given, in the case of the first pillar calculations based on the overburden load of the tributary area showed that the maximum average stress should be 219 ksc (i.e., greater than the measured 142 ksc)(25). Similar figures were not given for the other two pillars. However, it can be calculated that the overburden stress alone for the second pillar must have been 103 ksc and for the third pillar 120 ksc, both greater than the measured stresses.

Aside from the pillar measurements, an important observation made in this work was that by using the carrying capacity of the pillars for mine design the assumption is made that the roof can subside without breaking to the extent corresponding to the pillar loads (25). The implication is that there would be a sudden and probably drastic change in pillar loadings if the roof structure did break down.

The pillar measurements themselves in this work obviously are of questionable value (25). At the time that this research was done the state of the art was such that satisfactory bonding of the strain gauges to rock, and in particular to potash, was very difficult. Secondly, the effects of stress concentrations around the end of the borehole were ignored; the

calculated results would be changed considerably if this factor had been taken into account. Thirdly, as it is necessary in this technique to use the modulus of deformation of the ground, all the difficulties associated with determining the effective modulus of deformation of the rock mass would diminish the accuracy of the calculations. Moreover, potash is a rock whose modulus of deformation is particularly sensitive to strain rate, stress level, probably temperature, and probably the presence or absence of a confining pressure.

Other field work used the technique of prestressing a magneto-strictive pressure cell and then overcoring or relieving the cell. Measurements of the stresses in several pillars were made in a lead mine where the seam was lying horizontally (30). The depth of the workings was about 100 metres. The pillars were generally 8 to 9 metres in height and spaced 20 to 25 metres between centres. The extraction ratio was 90%.

The measured stresses were compared with the stresses calculated assuming that the entire overburden load resulting from the tributary area would be carried by the pillar (30). In one cluster of measurements the results indicated that the pillar nearest the abutment of the mining area was only carrying 16% of this maximum load whereas the pillar nearest the centreline of the mining area produced figures indicating stresses 125% of the maximum.

In another cluster of pillars it was again found that the lowest absolute stress occurred in the pillar nearest the abutment. The pillar closest to the centreline did not have the maximum measured stresses, but the stresses were not much below the maximum stresses occurring in an adjacent pillar somewhat farther from the centreline (31).

In this work the penetration of the pillars into the walls was considered; however, no use was made of this concept in attempting to provide a theoretical framework for the work (30).

Measurements in the abutments of the mining area indicated that the vertical stresses were roughly twice the magnitude of the overburden stress (30). This would be qualitatively consistent with a stress concentration effect modified by some plastic action associated with the semi-fractured ground close to the blasted faces.

However, stress measurements in the roof of the mining zone showed high compressive stresses and no tensile stresses (30). This by itself would indicate that the horizontal stresses would have to be greater than about 1/3 of the vertical stresses. The measurements within 2 metres of the roof line showed the horizontal major principal stress to be 4 to 12 times the vertical gravitational stress, with the intermediate principal stress being about $\frac{1}{2}$ of the major principal stress. It is probable that, within this distance,

stress concentration effects would produce principal stresses, and hence the measured quantities, greater than the field stresses.

Stress measurements were also made in a shaft pillar that was about 50 metres thick, 50 metres in breadth, and 170 metres long (30). The ore deposit was a magnetite dipping 60° to 75°, and the wall rocks were leptite and granite.

The measurements indicated that the horizontal field stress perpendicular to strike was of the order of 110 to 240 ksc, with the horizontal field stress parallel to strike being of the order of 280 to 360 ksc at a depth of 290 metres (30). At a depth of 185 metres, approximately in the centre of the pillar, the horizontal stress measurements in the pillar normal to the walls were of the order of 450 ksc.

These measurements will be examined later in the light of the proposed hypothesis of pillar loadings. The actual numbers have to be accepted with caution owing to the technical difficulties inherent in measuring the stresses, owing to the difficulty of determining from a few spot measurements the average stress in a pillar without knowing accurately the stress distribution, and owing to the inevitable influence of the varying lithological and structural features that provide the context for each individual set of measurements. These factors, of course, will apply to most field work of this nature.

In other work, an attempt was made to measure the changes in stress in pillars resulting from additional stoping (31). Glass stressmeters were used without overcoring; consequently, only relative measurements were obtained. The only useful conclusion from this work is that it showed that the direction of the major principal stress in pillars, as well as in undisturbed ground, could be influenced by the existence of a sloping ground surface such as would occur at the sides of a mountain. In other words, the major principal stress can be greater than the immediate overburden stress and can be inclined to the vertical.

Stress measurements were also made through several coal pillars with a borehole deformation metre using linear variable differential transformers as the transducers for measuring the changes in the borehole diameter (26). The instrument was used in a borehole approximately $1\frac{1}{2}$ inches in diameter which was overcored with a 10-inch diameter bit. The mining zone was approximately 480 feet below the surface, and it was stated that the pillars were in the centre of a large mined-out area. The measurements showed that the average pillar stresses were greater than the average stresses that would be calculated assuming the pillars were supporting the overburden load of the tributary area.

Some recent work on measuring changes in pillar strain during pillar recovery produced some unexpected results (76). The pillar

recovery operation was accompanied by caving in the old stopes. It was found that as the cave-line in these horizontal workings approached the instrumented pillars, the compressive vertical strain and the horizontal dilation or strain decreased. The reverse effect was expected. Then, in the light of these measurements, which were repeated for several measuring stations, a roof relaxation-arching-abutment mechanism was visualized. For this mechanism, the evidence of an abutment zone farther in from the cave-line was sought but was not found.

This phenomenon provides a good example of the usefulness of the new concept of pillar loading contained in this hypothesis. The mine plan shows that the span of the workings decreased towards the measuring stations (76). Consequently, it can be visualized that the deflection of the roof over the workings could be greater at the measuring stations when the cave-line was far away, owing to the greater span farther from the instrumented pillars inducing greater roof deflection at these pillars than when the cave-line approached the pillars and the roof deflection became less. With this decrease in roof deflection, of course, the pillar loadings would be decreased, producing the changes in vertical and horizontal strain that were actually measured.

Because the proposed hypothesis, which is established below, is based on deflection analyses, the theoretical and the empirical work on deflections that has been done by others can be examined. In some mathematical research, stress functions were established for various cases of bearing pressures to determine stress distributions (32). One of these cases was that of an internal elliptical crack. Based on this solution for the stresses around a crack in an infinite medium, the stresses, strains and displacements around a mining excavation, considered as a crack, were calculated and a general picture of the relative distributions obtained (33). The solutions were modified to take into account the presence of a horizontal free surface, the ground surface, at some distance above the crack and to include the compression of the abutments of the crack. The results were qualitatively similar to observed deflections.

It was considered in this work that the solutions were only valid for cases where L/z is less than about 0.7 (33). Also, they were limited to locations where hydrostatic field stresses occur.

The solutions also showed, apropos subsidence, that the point of maximum tension that occurs on the ground surface is not located at a constant angle from the abutment of the mining opening (33). In other words, a constant draw angle seems to be an invalid concept.

Again on deflections, but with the interest on subsidence, studies were conducted on gelatin models with L/z varying between 0.2 and 1.7 (34). Measurements of surface subsidence showed in all cases that the

subsidence vertically over the abutment line was approximately 50% of that obtained at the centre of the panel. This resulted from the strain distribution caused by the ground over the mining opening alone, as the abutments at the mining level being of steel were relatively incompressible.

Another theoretical solution for the subsidence of the ground surface due to underground mining deals with the case of isotropic ground (35). This solution is only applicable for the case where complete closure of the mining zone has occurred. When the theoretically predicted subsidence is compared with actual measurements, it is found that the actual subsidence is in excess of the theoretical prediction and that the effects of closure do not actually extend as far out horizontally as would be indicated by this theory.

This solution was later modified for a long excavation in transversely isotropic ground (36). In this case the predicted subsidence curve is in good relative agreement with some actual measurements. The solution was then further modified to take into account the third dimension of the mining geometry (37). This solution indicated that if the length of the mining panel was twice the breadth, the subsidence would be about 80% of that applicable to a long excavation for the case of plane strain. Consequently, it was concluded that the plane strain solution would be satisfactory for geometries where the length is more than twice the breadth of the mining opening.

An analysis by another worker of the measurements of surface subsidence at the centre of mining zones on several properties showed a variation with the ratio L/z (38). The maximum subsidence of about 84% of the thickness of the excavated seam was obtained when L/z was equal to or greater than 1.4.

In another review of subsidence measurements over horizontal coal workings, it was found that the settlement of the surface commonly showed the contribution of abutment compression (41). It was claimed that typical subsidence curves show downward movements over the edge of the panel varying between 15% and 25% of the maximum subsidence.

Underground measurements have been made in South Africa of closure in a hard rock stope as the span of the stope was increased (39). In addition, measurements were made in from the surface of the hangingwall to provide information on the source of closure. A pattern emerged that showed that the hangingwall expanded normal to the vein up to heights varying from 0.47 L to 0.91 L, with the coefficient of L increasing with span. It should be recognized that this expansion could result from tangential compression. Also from observations of the bulging of the face, it was judged that closure between the walls, or abutment compression, occurs even ahead of the face.

In addition, beyond a span of about 300 feet a contraction zone was detected in the immediate hangingwall (39). This was manifest by the distance between measuring points increasing initially with span and then contracting as the stoping span increased beyond 300 feet. This might be evidence of a decrease in tangential compression.

Another interesting investigation in hard rock was made at a depth below ground surface of 200 feet to 500 feet in a stope 10 feet to 12 feet high (40). The consequences of recovering pillars were measured. In one area, adjacent to a side abutment, the roof was bolted. Four pillars in the line adjacent to the abutment were removed, and a maximum convergence at this stage in the centre of the area of 0.142 inch was measured. These measurements will be analysed in a later section.

During the few hours after blasting these pillars the microseismic count increased to 20 to 30 cpm but within 24 hours the rate had returned to the normal background level of 1 to 5 cpm (40). The load on the bolts increased an average amount of 410 pounds during the week after blasting and then an average of 720 pounds during the seven weeks after blasting.

In a similar area, 125 feet x 125 feet, adjacent to a side abutment, by the time all the pillars were removed the maximum convergence was about 0.35 inch (40). Extensometer stations about 35 feet beyond the barrier pillars showed convergences of an average of 0.015 inch. This can be considered similar to abutment compression.

This abutment compression then increased to 0.046 inch, approximately 13% of the average convergence measured in the adjacent areas of pillar recovery when additional pillars were removed increasing the area of the zone to 125 feet x 200 feet. Most of the convergence occurred immediately on pillar removed, with an additional 10% occurring during the following week.

Again in a hard rock mine, closure between the hangingwall and footwall was measured as the face advanced in workings at a depth of about 4000 feet (42). The face was about 600 feet long on dip and was advancing on strike. It was found that by the time the face had advanced about 400 feet on strike the closure was about 1.7 feet.

Stimulated by these investigations a theoretical analysis of a long, horizontal slit in an infinite elastic medium was then produced (43). More recently this theory was extended to cover the general case of an inclined slit (44). The results of this general theory were then reduced for convenience to a graphical form (45). In this latter work the theoretical results were compared to underground displacement measurements with good agreement. As will be seen below, this deflection analysis is a

special case and in agreement with more general equations used below to develop the loading hypothesis.

Besides the above work pertinent to deep workings, the deflection of roof rock over horizontal workings with high values of L/z, or shallow depths, requires special examination. Some experimental work done to provide guidance for the design of deep concrete beams is of value in this connection (46). When L/z is greater than about 2.5 the straight-line distribution of bending stresses calculated in the conventional manner has been shown to be a valid representation of the actual distribution.

When L/z is smaller than about 2.5, it was found that the distance from the bottom edge of the beam to the centre of gravity of the tensile stress is constant and equal to about 0.06 L with a stress distribution similar to an opening in an infinite medium (46). In addition, the lever arm between the compressive and tensile bending forces was also found to become constant and equal to about 0.67 L, varying somewhat with the type of support and loading.

When L/z is less than about 1.4 in deep beams, it was found that the tensile force is constant and the extreme fibre tensile stress is equal to the uniformly distributed load on the beam. (These figures are all applicable to beams continuous over several supports (46).)

When L/z is less than 1, it was found that the neutral axis, or the point where the tensile stress changes to compressive stress, is fixed at an elevation equal to 0.20 L (46).

This information is useful as it provides guidance for determining where a beam analogy or hole analogy is more appropriate. For example, a hole in an infinite medium subjected to a vertical uniaxial stress field has a tangential tensile stress at the boundary of the hole at the top and bottom, and the magnitude of the tension varies little with the shape of the hole. This tangential tensile stress then decreases to zero at a distance into the material equal to about 0.2 L where L is the dimension of the hole in the direction normal to the direction of this field stress, similar to the findings for beams where L/z is less than 1.

Work based on theoretical studies of uniform loads applied to the tops of the beams with L/z of 0.5, 1 and 2, showed the neutral axes to be at 0.20, 0.25, 0.22 L respectively (47). For uniform loads applied at the bottom of the beam, the neutral axes were found to be at 0.23, 0.23 and 0.25 L.

Later photoelastic experiments showed that, for a centrally loaded beam when the depth was as great as the span, the deviation of the normal stresses from those calculated using the simple theory was not

great except close to the point of application of the load, where stress concentrations gave higher values, and along the top fibres where the normal stresses were essentially zero (48).

Photoelastic models loaded in a centrifuge gave experimental information on the stress distributions in beams with ratios of z/L up to 2.23. It was observed that for deep beams, the stresses are roughly equal to those of a beam with a depth (z') equal to span (L), the top part (z - z') merely providing additional load (49). These tests showed the neutral axis to lie 0.26 to 0.34 L above the bottom of the beam. The maximum tensile stresses seemed to vary from 0.75 to 1.23 of the loading pressure on the beam.

Some other experimental work with beams on elastic supports showed the importance of abutment compression in contributing to the deflection of the beam (50). This work also showed that the distribution of deflection was very close to that predicted from a beam analysis where the span was more than twice the depth of the beam.

Several theories have been conceived to provide an analytical basis for predicting the contribution to beam deflections of elastic abutments. These theories are based on the effect of the rotation of a cantilever at its support when the support consists of an infinite plate of the same material as the beam. Some experimental work was conducted to select the theory that best predicted the results (51). The experiments showed that at a distance from the support equal to 0.5 z, where z is the depth of the beam, the additional deflection was equal to about 100% of the calculated deflection assuming a rigid support. This obviously is a factor not to be ignored in any considerations based on deflections.

Other experiments that have some pertinence to rock masses with their joints and faults, were conducted to determine the effect of slots on the stress distribution in beams (52). Two slots of thickness 0.111 z, of depth 0.333 z and spaced 1.333 z apart, where z is the depth of the beam, were cut normal to the extreme fibre in a beam subjected to pure bending.

As was to be expected, there were high stress concentrations at the bottom of the slots (52). However, perhaps contrary to expectations, the measurements showed the existence of fairly high stresses tangential to the exterior surface in the material between the slots. These stresses varied from zero at the slots and approached a magnitude at the mid-point close to the value that would exist without the slots. In other words, this work suggests that the deflection of a beam with slots would be less than that of a beam where the material had been completely cut out between the slots. To support this view a complementary experiment, where the material between the slots was cut out, showed that the neutral axis was displaced upwards more than with slots alone and that the magnitude of the stresses resulting from bending were higher.

In examining the failure characteristics of masonry walls, some interesting data were also obtained on their deflection characteristics (53). It was found that masonry beams, which included a reinforced concrete sill beam, with L/z down to 1.25, produced deflections that were consistent with those computed using the theory of elasticity and taking into account the composite action of the different materials. It is useful as a rock mass analogue to have this confirmation that the deflections did vary for these deep beams with the moment of inertia of the cross-section. However, the difference between such a system and a rock roof is that the reinforced concrete sill beam provided a tension-resisting element, whereas in the case of a rock mass such tensile capacity might not exist.

As the proposed hypothesis of pillar loading will take into account the local penetration of the pillars into the walls, any substantiation of the theoretical prediction of the surface deflection resulting from a bearing load is of interest. Some information has been provided by measurements under large flexible steel tanks containing fluids (54). The substantiation of theory is only through the similarity of the shape of the surface deflection curve, rather than the magnitudes, as no independent measure of the modulus of deformation was obtained.

In other work, plate load tests were conducted to obtain information on prospective dam foundation rocks (55). The moduli of deformation obtained from the load tests varied from a low of 0.08 to a high of 0.6 of the moduli obtained from sonic velocity measurements on drill core obtained from holes at the same sites. In addition, measurements adjacent to these plates in the loading tests showed that the surface deflection was less than that predicted by elastic theory for a rigid die. Both results have some pertinence to the pillar problem.

On another project, five plate bearing tests with uniformly distributed pressure were conducted on rock faces (56). The deformation moduli for the five faces varied between 0.13 and 2.3×10^6 psi and were deduced from the equation $E = KP(1-\mu^2)/(Rs)$, where P is the applied load, R is the radius of the bearing surface, μ is Poisson's ratio (taken as 0.24), s is the deformation, and K is taken as 0.54 for a uniformly distributed load and 0.50 if the loading plate is rigid. No independently obtained moduli were available for appraising the accuracy of this technique. However, this type of test has been found to give valid results on concrete (57).

The variation with distance from the plate was also measured in this work and found to be different from that predicted by theory (56). At a certain distance from the centreline of the plate where theory would predict a deformation of about 20% of that measured on the centreline of the plate, the measurements showed this deformation to be about 4%. The jointing associated with the rock mass was considered to produce this deviation from the predicted deformation for a homogeneous elastic body.

Similar plate load tests were conducted in other work on three rocks: massive sandstone, basalt, and massive greywacke (58). Using the theoretical equation for the deflection of a flexible plate, the moduli of deformation were calculated as 24,700 psi, 36,900 psi and 74,000 psi. These figures all seem very low for the rocks involved. However, no information was given on the structural aspects; the rock may have contained many joints, possibly mud filled, as is common with near-surface bedrock.

Finally on the subject of pillar penetration into walls, from the results of a large number of plate load tests, from foundation strain measurements under dam loads, and from laboratory testing, it was concluded that the deformability during loading of a rock mass would be much higher if it had been subjected to adjacent blasting and had been permitted to decompress rather than if it was in its natural state (59). Comparison between moduli determined from in situ seismic velocities and plate load testing using the slope of the unloading curve were shown to agree very well, particularly on rocks that were not highly altered.

METHOD OF APPROACH

From the above review, it can be seen that no satisfactory theory exists for the calculation of pillar loads in horizontal workings nor in workings at other dip angles. Some measurements have been made which suggest that the tributary area theory often produces loads that are greater than actually occur. A start has been made, which can be continued, to take into account the structural aspects of the problem. These aspects are being increasingly recognized as important. Some work has been done on the stress distribution in pillars, on the deformation of mining areas, and on the local penetration of a loaded area into a rock surface, all of which can be of use in solving the loading problem.

The solution of the problem of how pillar loads can be predicted can be divided into two parts. The first part consists of solving the problem for elastic material. The second part consists of determining the significance of the deviation of the properties of rock masses from ideal elasticity.

The first problem must be solved by establishing a general analytical hypothesis that can be used for predicting pillar loads, or average stresses, for typical cases of room and pillar geometry. This hypothesis must then be tested using ideally elastic materials to either confirm or modify the hypothesis to develop a working theory. This procedure has been followed and will be described below.

The second part of the problem, that of determining the significance of the deviation of the properties of rock masses from those of elastic masses, can be examined to some extent with laboratory studies, but eventually this work must be supplemented with extensive field measurements of the stresses in pillars and in the surrounding ground.

It is often envisaged that roof rock is subjected to tensile stress and that this rock cannot sustain these stresses indefinitely as a result of the rock joints opening. The effect of this jointing in the roof rock on average pillar stresses can be examined in the laboratory in otherwise elastic material.

Also, it is probable that the result of removing the side constraint on pillar rock is to decrease its effective modulus of deformation. The effect of the pillar modulus of deformation being less than that of the walls can be examined in the laboratory.

Field stress measurements in pillars to compare with the predictions from the hypothesis must be made where the geometry is fairly regular and where the modulus of deformation can be determined without the difficulties of viscous or other reactions. Some measurements have been made by the Mines Branch, which, together with those made by others, are examined for their confirmation of or deviation from the equations established in the presently proposed hypothesis.

In defence of this approach it seems obvious that even though the geology of a site may compromise a theoretical solution, when no solution is available for even the ideal case the subject needs developing. Furthermore, a solution for the ideal problem could provide the practical man with a tool to obtain some guidance on such problems as the effects of changing the breadth of pillars, increasing the extraction ratio, going to greater depths, or working in different stress fields with otherwise similar ground and geometry.

HYPOTHESIS OF PILLAR LOADING

Long, Deep Mining Zone

Introduction. The previously established tributary area theory relating pillar stress only to the extraction ratio (6) has been, owing to the lack of any other theory, very useful. However, this theory is unsatisfactory in that the geometrical properties, such as the span or breadth of the mining zone with respect to its depth for horizontal workings, the height of the pillar, the breadth of the pillar and the pillar location within the mining zone, were all ignored. Also, such geological properties as the nature of the actual field stress, in particular the magnitude of the component parallel to the breadth of the mining zone, and the modulus of deformation of the pillar rock relative to that of the wall rocks, were not included.

In more recent work, attempts have been made to relate pillar loads to certain geometrical factors and rock parameters (11, 12, 15, 16). However, none of these attempts has produced comprehensive solutions to the problem, in that only some of the significant properties were included in each case.

Therefore, a general, comprehensive theory for the prediction of pillar loads is required. The following proposed hypothesis for the solution of this problem is based on solving the statically indeterminate net deflections of the walls. This net deflection at the pillars will be a measure of the increase in pillar stress resulting from mining. Although not all the complex factors have been included in this hypothesis, it does appear to contain most of the significant ones.

The deflection problem is solved by first establishing the equation for the deflection of a long, broad opening in an infinite medium. This is done by starting with the only case in which there is presently a comprehensive solution in plane stress or strain for the deflection of the boundary of an opening in an infinite mass - that of the circle. This solution contains the variables of location (i.e., the x-coordinate), normal and tangential field stresses (e.g., vertical and horizontal field stress for a horizontal seam), and the deformation properties of the material.

A solution is then derived for the deflection of the boundary of a hole in an infinite mass subjected only to a unidirectional pressure inside the hole. This deflection equation is compared with solutions of special cases for an ellipse. From this work more general deflection equations are postulated for the ellipse. These equations are compared

with special solutions obtained by other workers for crack or slit geometry and found to agree, providing some basis for assuming that the postulated general equation can be used for the geometry of mine workings in solving the problem of pillar loading.

It is then possible to calculate the inward wall deflection from relieving the constraint on the walls adjacent to the stopes or rooms by mining. The reverse deflection resulting from the average wall pressure from the pillar reactions can also be calculated. The net deflection resulting from these two actions should be the deflection of the pillars.

However, two additional mechanisms must be included. Excavation of the stopes eliminates the side pressure on the pillars, which will cause additional deflection along the length of the pillar. Also, the local penetration resulting from the concentration of the average wall pressure at the pillars will decrease the net deflection.

After the general solution has been established for deep workings, the special case of horizontal workings close to the ground surface is examined. In this case the deflection equations must take into account the finite distance to the ground surface or boundary. This is done by adapting existing theories and current experimental data for the deflection of structural elements similar in shape to the roof rock.

As a result of establishing this hypothesis, all the generally significant factors are functionally and quantitatively related to the increase in pillar loading produced by mining. Whereas in most cases this increase in loading will be less than that indicated by the tributary area theory, there can be cases where the loading would be greater than predicted by this theory. This arises from the deflection curve of the walls having a maximum at the centreline of the mining span which, of course, is greater than the average and may thus be greater than the loading that would be supplied by the immediate tributary area.

Tributary Area Theory. The tributary area (TA) theory assumes that each pillar will be loaded by the stress acting over the area of wall tributary to that pillar (6). For a long mining zone, or for the two-dimensional case, this can be expressed as:

$$\sigma_p = S_o (B_o + B)/B,$$

where σ_p is the average pillar stress, S_o is the field stress normal to the vein, B_o is the average breadth of the adjacent openings, and B is the breadth of the pillar.

For a series of rooms and pillars of equal dimensions the extraction ratio can be expressed as:

$$R = A_o/A_T = (N+1)B_o/((N+1)B_o + NB),$$

where A_o is the total wall area adjacent to the openings, A_T is the total wall area adjacent to the mining zone, and N is the number of pillars. Therefore

$$R = 1 - \frac{NB}{(N+1)B_o + NB}$$

$$= 1 - \frac{1}{\{(N+1)/N\}B_o/B + 1}.$$

But from above

$$\sigma_p/S_o = B_o/B + 1$$

$$= \frac{R}{1-R}\,\frac{N}{N+1} + 1 = \frac{1 - R/(1+N)}{1-R}$$

when $N \rightarrow \infty$ $\quad \sigma_p/S_o \rightarrow 1/(1-R)$.

This is the equation normally used in the TA theory; however, when N is small it gives an answer that is seriously in error with respect to the theory, e.g., for N = 1:

$$\sigma_p/S_o = \frac{R}{1-R}\,\frac{1}{2} + 1 = \frac{2-R}{2(1-R)}.$$

Therefore, the tributary area formula should be expressed as derived above

$$\sigma_p/S_o = \Delta\sigma_p/S_o + 1 = \frac{1 - R/(1+N)}{1-R} \qquad \text{Eq. 1(a)}$$

$$\text{or } \Delta\sigma_p/S_o = \frac{R}{1-R}\,\frac{N}{N+1} = \frac{R}{(1-R)(1+1/N)}. \qquad \text{Eq. 1(b)}$$

Deflection of a Circular Hole due to Applied Uniaxial Plane Stress. The deflection of the material around a circular hole in an infinite plate due to applied uniaxial stress in plane stress has been solved (61):

$$v_r = \text{radial displacement}$$

$$= \frac{S_o r}{2E}\left\{(1 + a^2/r^2) + (1 + 4a^2/r^2 - a^4/r^4)\cos 2\theta - \mu((1 - a^2/r^2) - (1 - a^4/r^4)\cos 2\theta)\right\},$$

where S_o = field stress,
r = radial distance to a point around the hole,
θ = angle from vertical to the radius vector passing through the point, and
E = modulus of elasticity of medium.

When $r = a$, the radius of the hole,

$$v_r = \frac{S_o a}{E}(1 + 2\cos 2\theta).$$

Similarly,

$$v_\theta = \text{tangential displacement}$$

$$= \frac{2 S_o a}{E}\sin 2\theta.$$

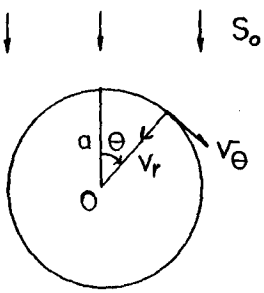

Figure 2. Deflection of a Circular Hole

It follows that the vertical displacement, δ, of a point on the circumference is

$$\delta = v_r \cos\theta + v_\theta \sin\theta$$

$$= \frac{S_o a}{E}(\cos\theta + 2\cos 2\theta\cos\theta + 2\sin 2\theta\sin\theta)$$

$$= 3 S_o a \cos\theta/E.$$

Deflection of a Circular Hole due to Excavation in Uniaxial, Plane Stress. The solution of this case does not seem to have been established before now. Here it is assumed that the deflections are small with respect to the size of the hole. Then

δ_1 = original vertical deflection with respect to O of a point in the medium on the circumference of a circular hole of radius a before the hole is excavated.

$$\delta_1 = S_o a \cos\theta/E.$$

From above,

δ_2 = total vertical deflection of a point on the circumference of the hole of radius a;

$\delta_2 = 3 S_o a \cos \theta / E.$

Hence, δ = vertical deflection due to excavation of the hole

$\delta = \delta_2 - \delta_1$

$\delta = 2 S_o a \cos \theta / E.$ Eq. 2(a)

Deflection of a Circular Hole due to an Internal Uniaxial Traction. This case also does not seem to have been solved. However, it now follows from the previous derivation. From Figure 3 it can be seen that the effect of excavation is equivalent to applying a stress around the circumference of the hole to produce a zero boundary stress. The increment of deflection resulting from excavation is thus the same as the deflection that would be caused by applying an internal traction on the boundary of a hole in an unstressed medium. Thus Equation 2 represents this case as well, i.e.,

$$\delta = 2 S_i a \cos \theta / E, \qquad \text{Eq. 2(b)}$$

where S_i = internal uniaxial traction in a circular hole.

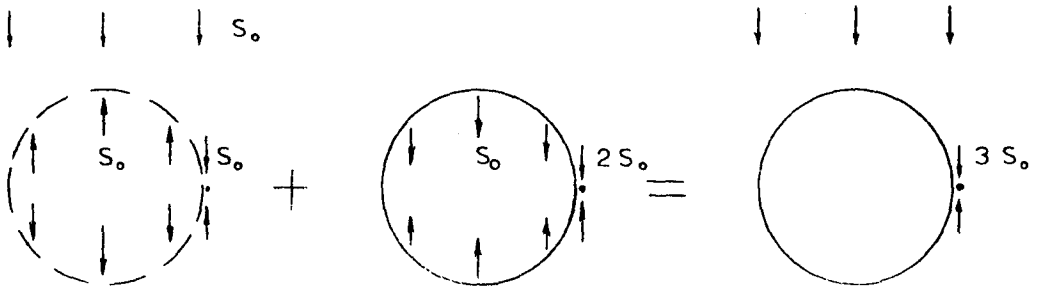

Figure 3. Stress Concentration from Internal Uniaxial Traction in a Circular Hole

Figure 3 also shows that the stress concentration in the wall of the hole, being $3S_o$, is made up of the original field stress, S_o, plus the effect of the excavation, $2S_o$. Hence it can be seen that the stress concentration due to an internal pressure produces a tangential stress, σ_t, in the walls at $\theta = \pi/2$:

$$\sigma_t = 2 S_i. \qquad \text{Eq. 3}$$

Deflection of a Circular Hole due to Applied Biaxial, Plane Stress. This case has been previously solved (61).

When r = a, the deflection of a point on the circumference is:

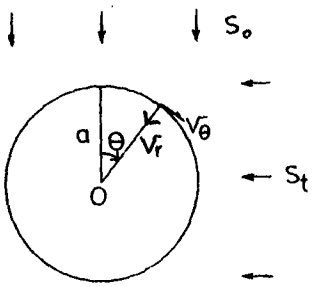

Figure 4. Deflection of a Circular Hole in Biaxial Plane Stress

$$v_r = \frac{r}{2E}\left\{(S_o+S_t)(1+a^2/r^2)+(S_o-S_t)(1+4a^2/r^2-a^4/r^4)\cos 2\theta\right\}$$

$$-\frac{\mu r}{2E}\left\{(S_o+S_r)(1-a^2/r^2)-(S_o-S_r)(1-a^4/r^4)\cos 2\theta\right\}$$

$$v_\theta = \frac{r}{2E}\left\{(S_o-S_r)(1+2a^2/r^2+a^4/r^4)\sin 2\theta\right\}$$

$$-\frac{\mu r}{2E}\left\{(S_o-S_t)(1-2a^2/r^2+a^4/r^4)\sin 2\theta\right\}.$$

The vertical deflection of a point on the circumference, following the same procedure as above for the uniaxial case, is:

$$\delta = v_r\cos\theta + v_\theta\sin\theta$$

$$\delta = \frac{a}{E}\left\{(S_o+S_t)\cos\theta + 2(S_o-S_t)\cos 2\theta\cos\theta + 2(S_o-S_t)\sin 2\theta\sin\theta\right\}$$

$$\delta = a(3S_o-S_t)\cos\theta/E. \qquad \text{Eq. 4}$$

Deflection of a Circular Hole due to Excavation in Biaxial, Plane Stress. This case has not previously been solved but follows from the above cases.

δ_1 = original vertical deflection with respect to O of a point in the medium before excavation

$\delta_1 = a(S_o - \mu S_t) \cos \theta / E$

δ_2 = total vertical deflection of a point around a hole, from Equation 4

$\delta_2 = a(3S_o - S_t) \cos \theta / E$

δ = deflection due to excavation of the hole

$\delta = \delta_2 - \delta_1$

$\delta = a(3S_o - S_t) \cos \theta / E - a(S_o - \mu S_t) \cos \theta / E$

$\delta = a(2S_o - S_t(1 - \mu)) \cos \theta / E$ Eq. 5(a)

Also, from Figure 5,

$$\cos \theta = \sqrt{(l^2 - x^2)}/l^2 = \sqrt{1 - (x'/l)^2}\,.$$

Hence $$\delta = l(2S_o - S_t(1 - \mu)) \sqrt{1 - (x'/l)^2}\,/E, \qquad \text{Eq. 5(b)}$$

or the vertical deflection due to an internal traction, S_i, is

$$\delta = l\,(2S_i - S_t(1 - \mu)) \sqrt{1 - (x'/l)^2}/E. \qquad \text{Eq. 5(c)}$$

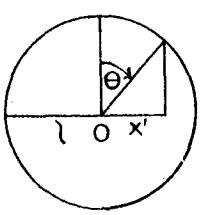

Figure 5. Geometrical Relations in a Circular Hole

Deflection Around an Elliptical Hole at $x' = 0$ due to Excavation in Hydrostatic Stress, Plane Strain with $\mu = 0.5$. This special case has been solved (62). As it is closer to the geometry of a mining opening, it is useful for comparison with the above solution for a circular hole. For $S_t = S_o$ the solution is

$$v_r = \delta = \frac{S_o a^2}{2G\sqrt{(y^2 + a^2 - b^2)}}$$

G = modulus of rigidity

$$= \frac{E}{2(1+\mu)} = \frac{E}{2(1+0.5)} = E/3.$$

When $y = b$

$$\delta = \frac{3S_o a}{2E}.$$

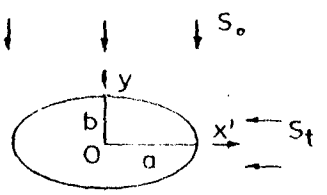

Figure 6. An Elliptical Hole in a Biaxial Stress Field

The comparable deflection of a circular hole in a hydrostatic stress field in plane strain, $\theta = 0$ and $\mu = 0.5$, can be obtained from Equation 5(a):

$$\delta = a(2S_o - S_t(1-\mu))\cos\theta/E.$$

To convert to plane strain, let $E \rightarrow E/(1-\mu^2)$ and $\mu \rightarrow \mu/(1-\mu)$ (63). Then

$$\delta = a\left\{2S_o - S_t\left(1 - \frac{\mu}{1-\mu}\right)\right\}\cos\theta\ \frac{(1-\mu^2)}{E}.$$

For $S_t = S_o$, $\theta = 0$ and $\mu = 0.5$,

$$\delta = 1.5\, S_o a/E.$$

This shows that the vertical deflection of a circular hole due to excavation, where $S_t = S_o$, $\theta = 0$ and $\mu = 0.5$, is the same as for an elliptical hole with its major semi-axis equal to the radius of the circular hole. This comparison, although for a special case, indicates that without a rigorous solution for the stope and pillar geometry, the circular opening might provide an expression that includes all the significant parameters. These parameters may thus function in a way that is a fair approximation to a stope and may give quantitative answers that are accurate for critical points, e.g., at the centre of the stope.

Deflection of an Elliptical Hole at $x' = 0$ due to Applied Uniaxial Stress, Plane Strain. Referring to Figure 6, the solutions for the two cases when $S_t = 0$ and when $S_o = 0$ have been given in the following form (62):

$$\frac{8G\delta}{S_o R} = \frac{2(d-1)}{m}\left[(m+1)\left\{\left(\frac{y}{2R}\right)^2 + m\right\}^{\frac{1}{2}} + \frac{y}{2R}\right]$$

$$+ \frac{1}{m^2}\left[\frac{m(m+1)^3}{\left\{\left(\frac{b}{2R}\right)^2 + m\right\}^{\frac{1}{2}}} + 2(m^2-1)\left\{\left(\frac{y}{2R}\right)^2 + m\right\}^{\frac{1}{2}} + 2(m^2+1)\frac{y}{2R}\right].$$

$$\frac{8G\delta}{S_t R} = \frac{2}{m}(d-1)\left[(m+1)\left\{\left(\frac{y}{2R}\right)^2 - m\right\}^{\frac{1}{2}} - \frac{y}{2R}\right]$$

$$+ \frac{1}{m^2}\left[\frac{m(1-m^2)(1-m)}{\left\{\left(\frac{b}{2R}\right)^2 - m\right\}^{\frac{1}{2}}} + 2(1-m^2)\left\{\left(\frac{y}{2R}\right)^2 - m\right\}^{\frac{1}{2}} - 2(1+m^2)\frac{y}{2R}\right],$$

where G is the modulus of rigidity, δ is the vertical deflection of points in the medium around the hole at $x = 0$, $R = (a+b)/2$, $d = 3 - 4\mu$, μ is Poisson's ratio, $m = (a-b)/(a+b)$ for the case $S_t = 0$, and $m = (b-a)(a+b)$ for the case $S_o = 0$.

For the vertical deflection of the boundary, i.e., $y = a$ at $x' = 0$, these equations can be reduced to the following form:

$$\frac{G\delta}{S_o} = (a + b/2)(1-\mu) \qquad \text{Eq. 6(a)}$$

$$\frac{G\delta}{S_t} = \frac{b}{2}(\mu - 1) \qquad \text{Eq. 6(b)}$$

The deflection of the boundary of an elliptical hole, δ_e, due to excavation can now be determined by subtracting from the deflections in Equations 6(a) and 6(b) the deflection that occurred before the excavation:

$$\frac{G\delta_e}{S_o} = (a + b/2)(1 - \mu) - \frac{b}{2}(1 - \mu)$$

$$= a(1 - \mu) \qquad \text{Eq. 7(a)}$$

and

$$\frac{G\delta_e}{S_t} = \frac{b}{2}(\mu - 1) - \left(\frac{-\mu b}{2}\right)$$

$$= -\frac{b}{2}(1 - 2\mu) \qquad \text{Eq. 7(b)}$$

As only elastic deflections are involved in this problem, the biaxial case in plane strain for the deflection of the boundary of an elliptical hole at $x' = 0$ can be obtained by adding the above two cases:

$$G\delta_e = S_o a(1 - \mu) - S_t b(1 - 2\mu)/2. \qquad \text{Eq. 7(c)}$$

Then as $E = 2G(1 + \mu)$, the equation can be changed to

$$\delta_e = \{2S_o a(1 - \mu^2) - S_t b(1 - \mu - 2\mu^2)\}/E. \qquad \text{Eq. 7(d)}$$

These equations can be compared to those for circular openings. From Equation 5(b) for $S_t = 0$ and plane stress

$$\delta = 2S_o t/E \quad \text{at } x' = 0.$$

Converting to plane strain by changing E to $E/(1 - \mu^2)$:

$$\delta = 2S_o t(1 - \mu^2)/E$$

Thus it can be seen that the magnitudes of the deflections for both cases - excavating a narrow ellipse and a circle - are equal at $x' = 0$ if the radius of the circle, t, is equal to the major semi-axis of the ellipse, a.

For the case of $S_o = 0$ the deflection of the circular hole at $x' = 0$ and in plane stress is, from Equation 5(b),

$$\delta = -S_t(1 - \mu)/E.$$

Converting to plane strain,

$$\delta = -S_t(1 - \mu - 2\mu^2)/E.$$

From this equation it can be seen that the magnitudes of the deflections in both cases of a narrow ellipse and a circle being excavated are equal at $x' = 0$ if the radius of the circle, l, is equal to the minor semi-axis of the ellipse, b.

As there is no solution yet available for the elliptical hole for $x' \neq 0$, it is possible that the solution for the circle may not be too different, particularly in view of the above comparisons, and could be used in the hypothesis and, if necessary, modified empirically.

Therefore, the equation for the deflection of the walls of a mining zone, as shown in Figure 8, following Equation 5(b), can be postulated from the equations for the circle and ellipse in plane stress using the semi-breadth in place of the semi-major axis of an ellipse or radius of a circle and h' in place of the semi-minor axis of an ellipse:

$$\delta = \{2 S_o l - S_t h' (1 - \mu)\} \sqrt{1 - (x'/l)^2}/E \qquad \text{Eq. 8(a)}$$

or

$$\delta = \{2 S_i l - S_t h' (1 - \mu)\} \sqrt{1 - (x'/l)^2}/E \qquad \text{Eq. 8(b)}$$

Comparison with Two Special Solutions. A solution based on previously established stress functions has been published, without derivation, for the deflection of a crack due to excavation in a hydrostatic stress field with $\mu = 0$ (32, 33). The vertical deflection of the boundary of the crack is given as follows:

$$\delta_K = \frac{S_o l}{G} \sqrt{1 - (x'/l)^2}$$

which can be converted to

$$\delta_K = 2 S_o l \frac{1 + \mu}{E} \sqrt{1 - (x'/l)^2}.$$

These equations apply to a condition of plane strain, and for the case $\mu = 0$:

$$\delta_K = \frac{2 S_o l}{E} \sqrt{1 - (x'/l)^2}.$$

The comparable deflection using Equation 8(a) would be

$$\delta = \{2 S_o l - S_t h' (1 - \mu)\} \sqrt{1 - (x'/l)^2}/E.$$

For $\mu = 0$ and $S_t = S_o$,

$$\delta = \{2S_o l - S_o h'(1-0)\}\sqrt{1-(x'/l)^2}/E$$

converting to plane strain $E \rightarrow E/(1-\mu^2)$

$$\delta = \{2S_o l - S_o h'\}\sqrt{1-(x'/l)^2}/E.$$

Then, if the definition of a crack is that $h'/l \rightarrow 0$,

$$\delta = \frac{2S_o l}{E}\sqrt{1-(x'/l)^2}$$

which is the same as that shown above for δ_K.

Another solution has been published for the deflection of a slit due to excavation in a uniaxial stress field in plane strain which is obtained from the following (43, 44, 45):

$$v_\rho = \frac{S_o l}{4G}\,\frac{(1+K)\rho^2\cos 2\alpha + 1 - K - 2}{\rho\sqrt{D}}$$

$$v_\alpha = \frac{S_o l}{4G}\,\rho\,\frac{(1-K)\sin 2\alpha}{\sqrt{D}}$$

where $D = \rho^4 - 2\rho^2\cos 2\alpha$, $K = 3 - 4\mu$.

Also, $x = \frac{l}{2}\,\frac{\rho^2+1}{\rho}\cos\alpha$, and $z = \frac{l}{2}\,\frac{\rho^2-1}{\rho}\sin\alpha$. ρ and α are curvilinear coordinates.

For $x'/l = 0$ and $\mu = 0.16$ the solution of the equations for the vertical deflection at the boundary of the slit gives (45):

$$\delta = \frac{3.36\,S_o l}{4G}.$$

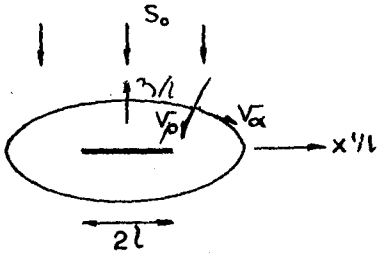

Figure 7. Deflection of a Slit in a Uniaxial Stress Field

This solution can be compared to that for a circular hole due to excavation in a uniaxial stress field, for plane strain, $\mu = 0.16$ and $x'/l = 0$, by using Equation 8(a):

$$\delta = (2S_o l - S_t h'(1 - \mu))\sqrt{1 - (x'/l)^2}/E.$$

Converting to plane strain and changing E to $2G(1+\mu)$,

$$\delta = 2S_o l \frac{(1-\mu^2)}{E} = 2\frac{S_o l (1-\mu^2)}{2G(1+\mu)}$$

$$= \frac{S_o l (1-\mu)}{G}.$$

For $\mu = 0.16$

$$\delta = \frac{0.84 S_o l}{G} = \frac{3.36 S_o l}{4G}.$$

This derivation for the special conditions applied to a slit also agrees with Equation 8(a). Furthermore, although no analytical expression was given for the distribution of the vertical deflection, numerical solutions given in graphs showed the same distribution with respect to x' as included in Equation 8(a).

The theory for the distribution of vertical deflection of a crack, slit or "infinitely thin crevice" has been previously established (75). It was shown that with a uniform internal pressure acting on the walls, the deformed shape was elliptical. It therefore follows that the vertical deflection, δ_x, at x' is related to that at the centre, δ_c, for a parallel walled slit:

$$\left(\frac{x'}{l}\right)^2 + \left(\frac{\delta_x}{\delta_c}\right)^2 = 1.$$

Therefore, $\delta_x/\delta_c = (1 - x^2)^{\frac{1}{2}}$ where $x = x'/l$. Curiously, this is the distribution, as shown above, to be expected for a circular hole.

Pillar Load and Average Stress from Deflections. The net pillar deflection, δ_p, will equal the algebraic sum of all the effects produced by the geology of the site and by mining. These are: the deflection of the potential pillar rock resulting from the field stresses, the deflection of the wall due to the release of stress, the deflection of the pillar due to release of side restraint, the reverse deflection of the wall due to the increased load applied by the pillar, and the local penetration of the pillar into the wall.

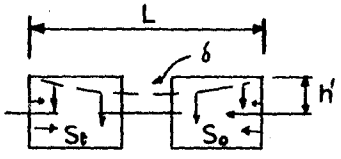

(a) δ is caused by the internal traction, S_o, over the walls adjacent to the individual rooms or by the average traction over the full breadth, L, of the mining zone, S_i, plus the similar action of S_t.

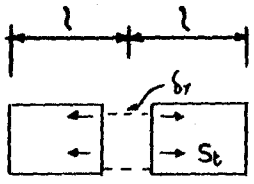

(b) δ_r is caused by the traction, S_t, on the sides of the pillar.

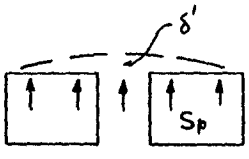

(c) δ' is caused by the increase in pillar stress, which produces the average pressure, S_p, over the area tributary to the pillar.

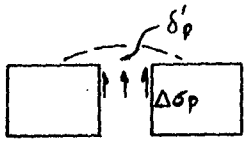

(d) δ'_p is the local penetration caused by the actual concentration of S_p into $\Delta\sigma_p$.

Figure 8. Deflection of a Pillar

The effects of mining only can be analysed to give the increase in the average stress in the pillar, with the total stress then being equal to the increase plus the original field stress. Thus the increment of pillar deflection, $\Delta\delta_p$, is related to the increase in pillar stress, $\Delta\sigma_p$:

$$\Delta\delta_p = \frac{\Delta P\, h'}{A_p E_p} = \frac{\Delta\sigma_p\, h'}{E_p}, \qquad \text{Eq. 9}$$

where $\Delta\delta_p$ is the increase in pillar deflection due to mining, ΔP is the increase in pillar load, h' is half the total height of the pillar, A_p is the horizontal cross-sectional area of the pillar, E_p is the modulus of deformation of the pillar rock, and $\Delta\sigma_p$ is the increase in the average pillar stress.

$$\text{Also,} \quad \Delta\delta_p = \delta - \delta_r - \delta' - \delta'_p ,$$

where $\Delta\delta_p$ is the deflection of the wall, assuming no pillar reaction due to the release of stress on the wall by excavating the openings; δ_r is the increase in deflection of the pillar under the original field stress resulting from the release of the side constraint; δ' is the reverse deflection of the wall resulting from $\Delta\sigma_p$; and δ'_p is the local penetration of the pillar into the wall. (Note: The above equation should include Δ's on the right side, but these are omitted for simplification. The Δ in $\Delta\delta_p$ is used to distinguish between the increase in pillar deflection due to excavation and the total deflection, δ_p, which includes the deflection in the ground before excavation.)

The deflection of the walls in a long mining zone can be calculated, consistent with material properties, using the special equations developed for either an ellipse (62), a crack (33), a slit (45), or the more comprehensive Equation 8(b) as established above:

$$\delta = \{ 2S_i \ell - S_t h' (1 - \mu)\} \sqrt{1 - (x'/\ell)^2}\,/E \qquad \text{Eq. 8(b)}$$

and $S_i = S_o A_o / A_T = R S_o$,
where A_o is the wall area exposed by mining, A_T is the total wall area adjacent to the mining zone, and R is the extraction ratio. Thus Equation 8(b) can be written:

$$\delta = S_o \ell \{2R - (S_t/S_o)(h'/\ell)(1 - \mu)\} \sqrt{1 - (x'/\ell)^2}\,/E. \qquad \text{Eq. 8(c)}$$

Equation 8(c) is for plane stress; however, the modifications for plane strain can be included in the final formulae. To fulfil the requirements of the above two-dimensional analysis, the length of the mining zone should be greater than twice the breadth and any section should be at least a distance from the ends of the mining zone equal to the breadth.

Equation 8(c) indicates that at $x'/\ell = \pm 1$, $\delta = 0$. This means there would be no compression of the abutments, which cannot be

true. To include abutment compression, the point A in Figure 9 can be assumed to deflect an amount equal to that of A', which is on the circumference of an imaginary circle with its centre at O and a radius of ℓ. This would give the same deflection as shown by Equation 5(c).

$$\delta_A = \frac{\ell}{E} (2S_i - S_t(1 - \mu)) \cos \theta'. \qquad \text{Eq. 10(a)}$$

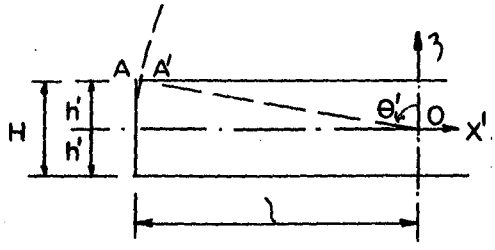

Figure 9. Approximation for Abutment Compression

The converting from a circle to a slot in the same way as was done to obtain Equation 8(a) is as follows:

$$\delta_A = \ell S_o (2R - (S_t/S_o)(h'/\ell)(1 - \mu)) (h'/\ell)/E. \qquad \text{Eq. 10(b)}$$

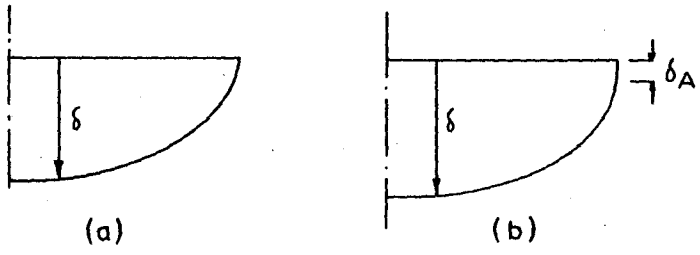

Figure 10. Deflection Curves With and Without Abutment Compression

Figure 10(a) shows the distribution $\delta(x)$ according to Equation 8(c). Figure 10(b) shows the abutment compression δ_A and is included in the hypothesis by adding Equations 8(c) and 10(b) to produce

$$\delta = \frac{S_o \ell}{E} \left(2R - \frac{S_t}{S_o} \frac{h'}{\ell} (1 - \mu)\right) \left(\sqrt{1 - (x'/\ell)^2} + h'/\ell\right). \qquad \text{Eq. 11}$$

The distribution $\delta(x)$ according to Equation 11 resembles empirical curves more closely than Equation 8(c), as abutment compression always occurs (33).

However, Equation 11 has not been established rigorously, although not illogically, and its value will depend entirely on empirical substantiation.

Reverse Deflection of Wall due to Average Pillar Pressure. From Equation 2(b), which may represent the deflection of a mining zone, in view of the similarities reviewed above between the solutions for a circle and a slit in an externally stressed medium, we have

$$\delta' = 2S_p \ell \cos\theta/E$$

$$\text{or } \delta' = 2S_p \ell \sqrt{1-(x'/\ell)^2}/E,$$

where S_p = the sum of the pillar loads divided by the sum of the individual tributary areas (i.e., the wall area occupied by the pillar plus that of the average adjacent opening).

The average increment in pillar stress, $\Delta\bar{\sigma}_p$, is the sum of the pillar loads (or the pillar pressure, S_p, multiplied by the sum of the tributary areas) divided by the sum of the pillar areas (parallel to the walls). Therefore, similar to Equation 1(b), it follows that

$$\Delta\bar{\sigma}_p = \Sigma\Delta P/\Sigma A_p = S_p/(1-R)(1+1/N)$$

$$\therefore \delta' = 2\ell\Delta\bar{\sigma}_p(1-R)(1+1/N)\sqrt{1-(x'/\ell)^2}/E.$$

Then to include the abutment decompression as was done for abutment compression in Equation 11:

$$\delta' = 2\ell\Delta\bar{\sigma}_p(1-R)(1+1/N)(\sqrt{1-(x'/\ell)^2}+h)/E. \quad \text{Eq. 12}$$

Distribution of Pillar Loads. Equation 12 is derived by starting with a uniform pressure. It is considered to give a good representation of the actual reverse deflection; however, an independent analysis can be made to establish the distribution of pillar loads without making the above assumption. The deflection of a circular inclusion welded to the medium has been solved for the uniaxial case shown in Figure 11 in the following form (43):

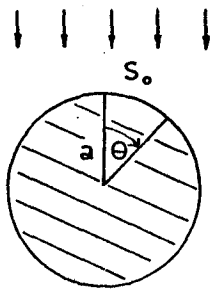

Figure 11. Circular Inclusion in a Uniaxial Stress Field

$$v_r^i = \frac{S_o r}{8 G_i} \beta_i (d_i - 1) + (\gamma_i (d_i - 3) r^2/a^2 + 2D_i) \cos 2\theta$$

$$v_\theta^i = \frac{S_o r}{8 G_i} (\gamma_i (d_i + 3) r^2/a^2 - 2D_i) \sin 2\theta$$

where β, γ and D are constants; $d = 3 - 4\mu$ for plane strain; symbols with subscript i refer to the inclusion, and those with no subscript refer to the medium. From the boundary conditions of the inclusion, it follows that

$$\beta_i = \frac{G_i (d + 1)}{2 G_i + G(d_i - 1)}, \quad \gamma = 0, \quad D_i = \frac{G_i (d + 1)}{G + G_i d}.$$

Because pillars provide a reaction normal to the walls only, we can use $\mu_i = 0$. Then at the boundary of the inclusion, the displacements will be:

$$v_r = \frac{S_o a}{8 G} (\beta_i (d_i - 1) + 2D_i \cos 2\theta)$$

$$d = 3 - 4\mu$$

$$d_i = 3 - 0 = 3$$

$$\beta_i = \frac{G_i (3 - 4\mu + 1)}{2G_i + G(3 - 1)} = \frac{2 G_i (1 - \mu)}{G_i + G}$$

$$D_i = \frac{G_i (3 - 4\mu + 1)}{G + G_i (3 - 4\mu)} = \frac{4 G_i (1 - \mu)}{G + G_i d};$$

$$\therefore v_r = \frac{S_o a}{8 G_i} \left(\frac{2G_i (1 - \mu)^2}{G_i + G} + \frac{2G_i (1 - \mu) \cos 2\theta}{G + G_i d} \right)$$

$$= \frac{S_o (1 - \mu) a}{2} \left[\frac{1}{G_i + G} + \frac{2 \cos 2\theta}{G + G_i d} \right]$$

$$v_\theta = -\frac{S_o a}{8 G_i} \left[-2 \frac{4G_i (1 - \mu)}{G + G_i d} \right] \sin 2\theta$$

$$= S_o a \frac{(1 - \mu) \sin 2\theta}{G + G_i d}.$$

For an applied stress perpendicular to S_o:

$$v_r = \frac{S_t(1-\mu)a}{2}\left[\frac{1}{G_i+G} + \frac{2\cos(-2(\pi/2-\theta))}{G+G_id}\right]$$

$$= \frac{S_t(1-\mu)a}{2}\left[\frac{1}{G_i+G} - \frac{2\cos 2\theta}{G+G_id}\right]$$

$$v_\theta = \frac{S_t a(1-\mu)}{G+G_id}\sin(-2(\pi/2-\theta))$$

$$= -\frac{S_t a(1-\mu)}{G+G_id}\sin 2\theta.$$

Hence, for a biaxial case:

$$v_r = \frac{a}{2}\left[\frac{(S_o+S_t)(1-\mu)}{G_i+G} + \frac{2(S_o-S_t)(1-\mu)}{G+G_id}\right]\cos 2\theta$$

$$v_\theta = \frac{S_o - S_t a(1-\mu)}{G+G_id}\sin 2\theta.$$

Thus the vertical deflection for the biaxial case is:

$$\delta'' = v_r\cos\theta + v_\theta\sin\theta$$

$$= a(1-\mu)\left[\frac{(S_o+S_t)\cos\theta}{2(G_i+G)} + \frac{(S_o-S_t)\cos 2\theta\cos\theta}{G+G_id} + \frac{(S_o-S_t)\sin 2\theta\sin\theta}{G+G_id}\right]$$

$$\delta'' = a(1-\mu)\cos\theta\left[\frac{S_o+S_t}{2(G_i+G)} + \frac{S_o-S_t}{G+G_id}\right]$$

From this equation it can be seen that

$$\delta'' \propto \cos\theta$$

$$\propto \sqrt{1-(x'/t)^2}$$

Hence as the increment in pillar stress varies with the deflection

$$\Delta\sigma_p \propto \sqrt{1-(x'/t)^2}$$

It is then possible to relate $\Delta\sigma_p$ to $\Delta\bar{\sigma}_p$, in view of the maximum value, $\Delta\sigma_{p\text{-}max}$, occurring at $x' = 0$:

$$\Delta\bar{\sigma}_p = \Delta\sigma_{p\text{-}max} \int_0^1 \sqrt{1 - (x'/l)^2}\, d(x'/l)$$

$$= \Delta\sigma_{p\text{-}max} \left[\frac{x'}{2l} \sqrt{1 - (x'/l)^2} + \tfrac{1}{2} \sin^{-1} x'/l \right]_0^1$$

$$= \frac{\pi}{4} \Delta\sigma_{p\text{-}max}$$

$$= \frac{\pi \Delta\sigma_p}{4\sqrt{1 - (x'/l)^2}} .$$

Substituting in Equation 12

$$\delta' = \frac{2\pi \Delta\sigma_p (1 - R)(1 + 1/N)\, l\, (\sqrt{1 - (x'/l)^2} + h)}{4E\sqrt{1 - (x'/l)^2}}$$

$$= \frac{\pi \Delta\sigma_p (1 - R(1 + 1/N)(1 + h/\sqrt{1 - (x'/l)^2})}{2E} \qquad \text{Eq. 13}$$

Local Penetration of Pillars into the Walls. Instead of having an average pressure, S_p, applied to the walls by the pillars, there is a concentration of pressure or stress, $\Delta\sigma_p$, at the pillars which causes local penetration in excess of the general reverse deflection δ'. A solution exists for the relative penetration, δ, due to a uniform pressure on the edge of a semi-infinite plate (64):

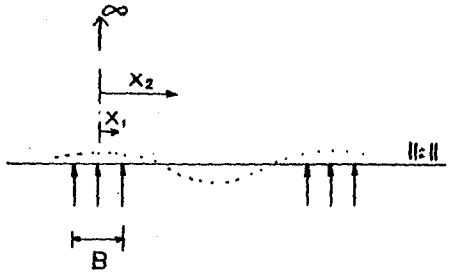

Figure 12. Deflection of the Edge of a Semi-Infinite Plate

$$\delta = \frac{2\sigma}{\pi E}\left\{(B+2x_1)\ln\frac{2x_2-B}{B+2x_1} + (2x_2-B)\ln\frac{2x_2-B}{B-2x_1}\right\} + \frac{\sigma B(1-\mu)}{\pi E} \qquad \text{Eq. 14(a)}$$

where σ = uniform pressure on the edge of the plate,

B = width of the loaded zone,

x_1 = distance from ℄ of load, within the loaded zone, to the point where δ occurs, and

x_2 = distance from ℄ of load, beyond the loaded zone to the point to which δ is related.

As will be shown later, theoretically the local penetration will affect the calculated pillar stress by an amount varying from nil to slight. Furthermore, it is probable that empirically the importance of B owing to other mechanisms may require an alteration of its coefficient based on experimental data. (E.g., with varying sizes of pillars the pillar loads are likely to vary with x somewhat differently than $\Delta\sigma_p$ does, hence δ' is likely to be greater than calculated at large pillars; also the effective modulus of deformation may vary with B.) Therefore, an arbitrary but simple case is used to obtain a coefficient for Equation 14(a): $x_1 = 0$ and $x_2 = B$. This coefficient may be altered empirically. Hence, the maximum local penetration with respect to a point at a distance from the side of the pillar equal to B/2 due to the excess of $\Delta\sigma_p$, the concentrated stress, over the average pressure, S_p, is:

$$\delta'_p = \frac{\Delta\sigma_p - S_p}{\pi E} B(1-\mu)$$

$$= \left\{\Delta\sigma_p - \frac{\Sigma(\Delta\sigma_p B)}{L}\right\}\frac{B}{\pi E}(1-\mu)$$

$$= \Delta\sigma_p\left\{1 - \frac{\Sigma(B)}{L}\right\}\frac{B}{\pi E}(1-\mu)$$

$$= \Delta\sigma_p(1-(1-R))\frac{B}{\pi E}(1-\mu)$$

$$\delta'_p = \frac{\Delta\sigma_p BR}{\pi E}(1-\mu). \qquad \text{Eq. 14(b)}$$

The use of Equation 14(a) for this mechanism, rather than one giving an absolute measure of penetration, has an additional advantage in that, by restricting the relative penetration to that for the area within

a distance B/2 on either side of the pillar, the pattern is consistent with experimental results. These results show that the settlement crater is restricted to a much smaller area surrounding the loaded area in rock than would theoretically apply to a continuous elastic mass (55, 56).

Pillar Formula Resulting from Deflection Hypothesis. The pillar load can be obtained by substituting Equations 11, 13, 14(b) and the appropriate expression for δ_r into Equation 9:

$$\frac{\Delta P h'}{A_p E_p} = \frac{S_o t}{E}\left(2R - \left(\frac{S_t}{S_o}\right)\left(\frac{h'}{t}\right)(1-\mu)\right)\left(\sqrt{1-(x'/t)^2} + h'/t\right) - \frac{\mu_p S_t h'}{E_p}$$

$$- \frac{\pi \Delta\sigma_p t}{2E}(1-R)(1+1/N)\left(1+h/\sqrt{1-(x'/t)^2}\right) - \frac{\Delta\sigma_p RB}{\pi E}(1-\mu)$$

$$\therefore \Delta P = S_o A_p \left\{\frac{(2R-(S_t/S_o)(h'/t)(1-\mu))\left(\sqrt{1-(x'/t)^2}+h'/t\right)-\mu_p(S_t/S_o)(h'/t)(E/E_p)}{(h'/t)(E/E_p)+\pi(1-R)(1+1/N)\left(1+h/\sqrt{1-(x'/t)^2}\right)/2+R(B/t)(1-\mu)/\pi}\right\},$$

$$\frac{\Delta\sigma_p}{S_o} = \left\{\frac{(2R-(S_t/S_o)(h'/t)(1-\mu))\left(\sqrt{1-(x'/t)^2}+h'/t\right)-\mu_p(S_t/S_o)(h'/t)(E/E_p)}{(h'/t)(E/E_p)+\pi(1-R)(1+1/N)\left(1+h/\sqrt{1-(x'/t)^2}\right)/2+R(B/t)(1-\mu)/\pi}\right\}. \quad \text{Eq. 15(a)}$$

To convert Equation 15(a) to plane strain from plane stress, change all E's to $E/(1-\mu^2)$ and all μ's to $\mu/(1-\mu)$. Then, to simplify, let

$$M = E/(1-\mu^2) \qquad b = B/L$$
$$w = \mu/(1-\mu) \qquad x = x'/t$$
$$k = S_t/S_o \qquad h = h'/t$$
$$n = M/M_p$$

$$\therefore \frac{\Delta\sigma_p}{S_o} = \frac{(2R - kh(1-w))\left(\sqrt{1-x^2}+h\right) - w_p khn}{hn + \pi(1-R)(1+1/N)\left(1+h/\sqrt{1-x^2}\right)/2 + 2Rb(1-w)/\pi} \quad \text{Eq. 15(b)}$$

Then $$\sigma_p/S_o = \Delta\sigma_p/S_o + 1. \quad \text{Eq. 15(c)}$$

Equations 15 and 15(c) will reduce to equations that are similar to the tributary area theory when $k = 0$, $x = 0$, $h \longrightarrow 0$, and $b \longrightarrow 0$. The only remaining difference arises from the different coefficients in the numerator $(2R)$ and denominator $(1-R)\pi/2$, neglecting the inclusion in

Equations 15 and 15(c) of the variation of σ_p with x. The difference in coefficients arises from recognizing the shape of the wall deflection curve, which results in greater than average pillar loads at the centre of the span and less than average towards the abutments.

Long, Shallow Mining Zone

Introduction. When the mining zone of horizontal workings is close to the surface in relation to its breadth, or z/L becomes small, then the equations formulated for an infinite medium can no longer be used for determining the deflection of the walls. The analysis of the deflection of the roof is then more accurately done using a deep beam analogue. An equation must be established to give the deflection of the under surface of a deep beam restrained by elastic supports.

Below, an equation is obtained for this case, which is then used to determine the deflections due to removing the constraint provided by the excavated ground. The reverse deflection due to the average wall pressure resulting from the increase in pillar stress can also be calculated using this equation. The ultimate deflection again includes the results of removing the side constraint from the pillar and the local penetration of the pillar into the walls.

For the long, shallow mining zone, although the stress distribution in the roof rock is affected by the nearness of the surface, that of the floor rock is only slightly altered from the infinite medium case. Consequently, the net closure of the mining zone, being the sum of the net deflection of the roof and of the floor, must be determined by considering separately the mechanics of the floor and roof. This net closure is a measure of the increase in pillar stress.

Deflection of a Restrained Beam. A special case arises when the mining zone is either close to the ground surface or very broad compared to its depth, in other words when L/z becomes large. In this case, when the mining zone is horizontal, the roof can no longer act in a manner equivalent to that over an opening in an infinite medium. The proximity of a boundary, the ground surface, significantly alters the strain distribution in the overlying ground. It has been found that when L/z is greater than 2 the variation of the horizontal stress, σ_x in beams is substantially straight-line as in simple beam theory, depending to some extent on types of loading and support (46). Furthermore, when L/z is greater than 1.25, experiments show that deflections can be calculated using normal beam theory (53).

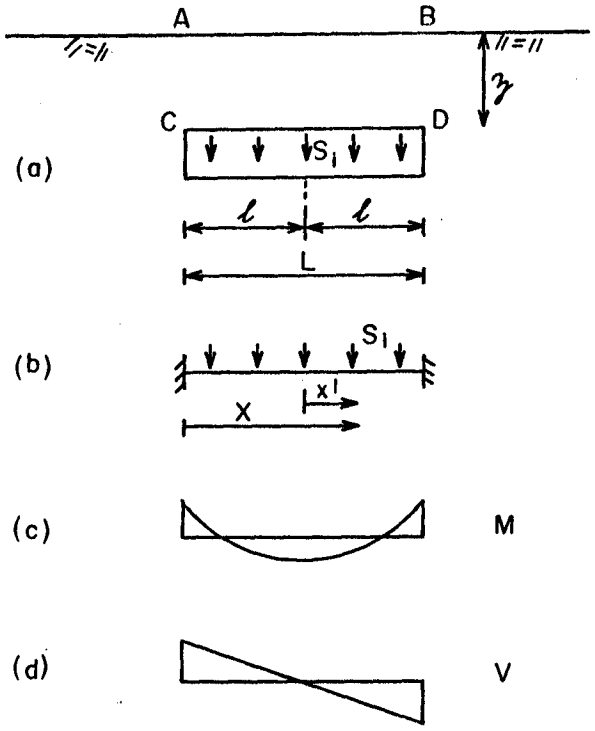

Figure 13. A Long, Shallow Mining Zone

When L/z becomes less than 1 the variation of σ_x approaches that of an opening in an infinite medium. The neutral axis is located at a constant distance from the bottom surface of about 0.2 L, and the maximum σ_x becomes constant and approximately equal to the average external loading plus the weight of the beam (47, 48). In addition, photoelastic studies have shown that as z is increased with a constant L for L/z less than 1, the only change in stress is that which would result from adding a load equal to the weight of the additional depth of the beam (49).

Therefore, where L/z is less than 1 Equation 11 should predict δ, i.e., by assuming the opening is in an infinite medium, whereas for L/z greater than 1 a beam analysis should be more accurate for the deflection of the roof. However, for the floor it has been shown by experiment that the stress distribution around the side of a hole away from the planar boundary changes very little as the hole approaches the boundary (65). Therefore, Equation 15 should represent the deflection of the floor for all cases.

Assuming, in Figure 13(a), that the roof rock ABCD has the stress distribution and deformation similar to those of a beam, the deflection

resulting from excavating the mining zone will be that of a restrained beam with the distributed load per unit width of S_i, i.e., excavating is equivalent to adding the stress S_o at the roof line, which cancels out the initial stress and leaves a boundary free of constraint over the rooms (note: as before $S_i = R S_o$).

Assuming the ends AC and BD are restrained from rotating, the beam will be equivalent to that shown in Figure 13(b), with a moment diagram as shown in Figure 13(c), and a shear diagram as shown in Figure 13(d).

The deflection of the neutral axis due to pure bending, δ_b, of the beam shown in Figure 13 is found from the usual equation:

$$\delta_b = \frac{S_i X^2}{24 E I} (L - X)^2$$

$$\delta_b = \frac{S_i x^2}{2E} (1 - x)^2 (l/z)^3 l, \qquad \text{Eq. 16}$$

where $x = x'/l$.

The deflection of the beam shown in Figure 13 due solely to shear stresses can be derived using the following expression (64):

$$\delta_s = 1.2 \int \frac{V v \, dx}{A G},$$

where V is the shear force in the beam, v is the shear force due to a unit load acting at the section where the deflection is being determined, A is the area of the vertical section, and G is the modulus of rigidity. The integration must extend over the full length of the beam, L, with βL defining an intermediate point and equal to X as shown in Figure 14.

$$\delta_s = \frac{1.2}{zG} \left\{ \int_0^{\beta L} (S_i L/2 - S_i X)(1 - \beta) dX + \int_{\beta L}^{L} (S_i L/2 - S_i X)(-\beta) dX \right\}$$

$$\delta_s = \frac{0.6 S_i}{G} \beta (1 - \beta)(L/z) L$$

$$= \frac{0.6 S_i}{G} (1 - x^2)(l/z) l. \qquad \text{Eq. 17}$$

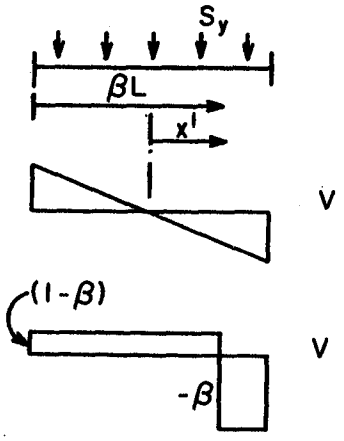

Figure 14. Coordinates for Deflection Calculation

Equations 16 and 17 both provide the deflections of the neutral axis of the beam. However, we are concerned with the deflections of the underside. The deflection of the roof of the excavation shown in Figure 13(a) will be greater than that of the neutral axis, owing to the expansion of the ground resulting from the actual release of stress by the excavation. The changes in stresses caused by the load shown in Figures 13(a) and 13(b) are as follows (66):

$$\sigma_x = \frac{3S_i z'}{4(z/2)^3}(\ell^2 - x'^2) + \frac{S_i z'}{2(z/2)^3}\left\{z'^2 - \frac{3(z/2)^2}{5}\right\} - \frac{S_i z'}{2(z/2)}\left\{\frac{\ell^2}{(z/2)^2} - \frac{3}{5} - \frac{3\mu}{2}\right\}$$

$$\sigma_z = \frac{S_i z'}{4(z/2)^3}(3(z/2)^2 - z'^2) + \frac{S_i}{2}.$$

Therefore, the deflection of the lower surface of the beam shown in Figure 15 with respect to the neutral axis is:

$$\delta_e = \frac{1}{E}\int_0^{z/2} (\sigma_z - \mu\sigma_x)\, dz'$$

$$= \frac{S_i z}{32 E}\left\{13 - 2\mu(12(\ell^2 - x'^2)/z^2 + 1 - 8\ \ell^2/z^2 + 3\mu)\right\}$$

$$= \frac{S_i z}{32 E}\left\{13 - 2\mu(12(1 - x^2)(\ell/z)^2 + 1 - 8\,(\ell/z)^2 + 3\mu)\right\}. \qquad \text{Eq. 18}$$

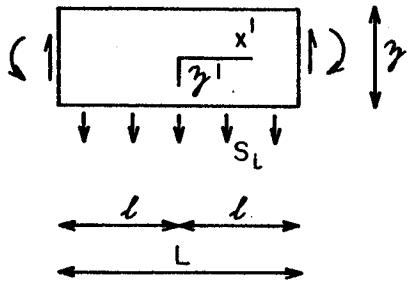

Figure 15. Free Body Diagram of Roof Rock

If the beam material is continuous with that of the support, the support itself will be elastic and not rigid as assumed in deriving normal beam equations. The elasticity of the support requires that the stresses and deformations or strains be compatible, which is not fulfiled by assuming a straight-line variation of strain. It has been found experimentally that the rotation at an elastic support due to the moment, M, is for a plane stress condition (51):

$$\theta = \frac{16.67\,M}{\pi E z^2} \qquad \text{Eq. 19}$$

For a fixed beam this is equivalent to applying an added moment, M_e, at the supports of opposite sign to the calculated fixing moment, M_f. From the area-moment theorem, the relations between M_e and M_f can be established. The actual bending moment at the supports is:

$$BM = M_f - M_e$$

$$\therefore \theta = \frac{16.67\,(M_f - M_e)}{\pi E z^2}.$$

But by superposition, the rotation of the supports by M_e could occur first. Thus, as shown in Figure 16(e),

$$\theta_{AB} = \frac{M_e\,\ell}{EI}.$$

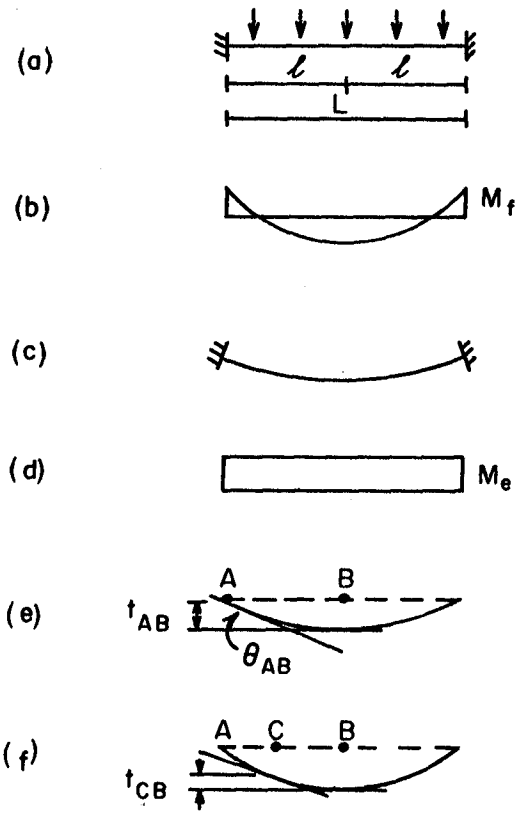

Figure 16. Deflection of Beam with Elastic Supports

Combining the two equations for θ gives

$$\theta = \frac{16.67\,M_f}{\pi E z^2}\left\{1 - \frac{1}{\frac{12\pi}{16.67}\frac{t}{z} + 1}\right\} \qquad \text{Eq. 20}$$

or

$$\theta = \frac{16.67\,M_f}{\pi E z^2} \cdot F$$

where $F = 1 - \dfrac{1}{\frac{12\pi}{16.67}\frac{t}{z} + 1}$.

The additional deflection of the beam due to the rotation of the supports, δ_c, can be determined also using area-moment theorems. From Figures 16(e) and 16(f) it can be seen that

$$\delta_c = t_{AB} - t_{CB},$$

where t is the intercept between the tangents at two points that have deflected due to M_e. It is known that

$$t_{AB} E I = \int_0^{l} M_e X \, dx$$

$$= M_e l^2/2$$

$$\text{and } M_e = \theta_{AB} E I / l$$

$$= \frac{16.67 M_f F}{\pi E z^2} \frac{E I}{l}$$

$$= \frac{16.67 F}{3 \pi E} \frac{S_i l}{z^2} E I$$

$$\therefore t_{AB} = \frac{16.67 F}{6 \pi E} \frac{S_i l^3}{z^2} .$$

Similarly, referring to Figure 16(f) and with the origin at the ℄ of the opening, it follows that:

$$t_{CB} E I = M_e x'^2/2$$

$$\text{or} = M_e l^2 x^2/2.$$

$$\therefore t_{CB} = \frac{16.67 F}{6 \pi E} \frac{S_i l^3}{z^2} x^2$$

$$\therefore \delta_c = \frac{16.67 F}{6 \pi E} \frac{S_i l^3}{z^2} (1 - x^2)$$

$$= \frac{0.884 F S_i l^3}{E z^2} (1 - x^2). \qquad \text{Eq. 21}$$

$$\delta = \delta_b + \delta_s + \delta_e + \delta_c$$

$$= \frac{S_i \ell}{2E}\left(\frac{\ell}{z}\right)^3 (1-x)^2 + \frac{0.6\, S_i \ell}{G}\,\frac{\ell}{z}\,(1-x^2)$$

$$+ \frac{S_i z}{32E}\,(13 - 2\mu(12(1-x^2)(\ell/z)^2 + 1 - 8(\ell/z)^2 + 3\mu))$$

$$+ \frac{0.884\, F\, S_i \ell}{E}\left(\frac{\ell}{z}\right)^2 (1-x^2)$$

$$= \frac{S_i \ell}{E}\,(C_b/z'^3 + C_s/z' + C_e z' + C_c/z'^2) \qquad \text{Eq. 22}$$

where $C_b = (1-x)^2/2$,

$C_s = 0.6\,(1-x^2)E/G = 1.2(1-x^2)(1+\mu)$,

$C_e = (13 - 2\mu((12(1-x^2)/z'^2 + 1 - 8/z'^2 + 3\mu))/32$,

$F = 1 - (1/(2.26/z' + 1))$, and

$z' = z/\ell$.

Reverse Deflection of Roof due to Average Pillar Pressure. Following the procedure used for the hole in an infinite medium, the reverse deflection due to the average pillar pressure, S_p, can be determined using Equation 22:

$$\delta' = \frac{S_p \ell}{E}\,(C_b/z'^3 + C_s/z' + C_e z' + C_c/z'^2)$$

$$\text{or } \delta' = \frac{\Delta\bar{\sigma}_p \ell (1-R)(1+1/N)\,(f(x)+h)}{E}\,K_b$$

where $K_b = C_b/z'^3 + C_s/z' + C_e z' + C_c/z'^2$, and

$f(x) = 1 - x^2$ as will be determined below.

Distribution of Pillar Loads. The variation of pillar loads with position will be, as for the previous case, the same as the variation of the roof and floor deflection, δ. To establish an expression for the variation of the roof deflection similar to Equation 5(b), the individual components of Equation 22 must be examined.

The relative magnitudes of δ_b, δ_s, δ_e and δ_c are calculated for the centre of the range where Equation 22 is likely to be more valid than

Equation 11. For this purpose let $z' = 1$, $x' = 0$ and $\mu = 0.2$. From Equations 16, 17, 18 and 21,

$$\delta_b = 0.500\, S_i/E \qquad \delta_s = 1.440\, S_i/E$$
$$\delta_e = 0.348\, S_i/E \qquad \delta_c = 1.660\, S_i/E$$

and when $z' = 2$:

$$\delta_b = 0.062\, S_i/E \qquad \delta_s = 0.720\, S_i/E$$
$$\delta_e = 0.748\, S_i/E \qquad \delta_c = 0.415\, S_i/E$$

It can be seen that, over the range in which Equation 22 is most likely to be of use, δ_s is the most significant followed by δ_c and δ_e.

To examine the variation with x of δ_s, δ_e and δ_c, Equations 17, 18 and 21 can be rewritten as follows:

$$\delta_s = K(1 - x^2)$$
$$\delta_e = K' \left\{13 - 2\mu(12(1 - x^2)/z'^2 + 1 - 8/z'^2 + 3\mu)\right\}$$
$$\delta_c = K''(1 - x^2).$$

For $z' = 2$ and $\mu = 0.2$, $\delta_e = 11.96\, K'$ when $x' = 0$. The variations with x are shown numerically as follows:

	x = 0	0.1	0.2	0.5	0.8
δ_s/K	1	0.99	0.96	0.75	0.36
$\delta_e/(11.96\, K')$	1	1.00	1.02	1.025	1.07
δ_c/K''	1	0.99	0.96	0.75	0.36

This table shows that δ_e varies little with x. Thus for a first approximation, and recognizing that the variations of δ_b and δ_e will largely cancel each other, the variation of δ and hence $\Delta\sigma_p$ will be according to the function $(1 - x^2)$. Hence it follows that:

$$\Delta\sigma_p = \Delta\sigma_{p\text{-}max}(1 - x^2)$$

$$\text{and} \quad \Delta\bar{\sigma}_p = \frac{\Delta\sigma_{p\text{-}max}}{t} \int_0^t (1 - x^2)\,dx'$$

$$= 0.667\,\Delta\sigma_{p\text{-}max}$$

$$\therefore \quad \Delta\sigma_p = \frac{3\,\Delta\bar{\sigma}_p}{2}(1 - x^2)$$

$$\therefore \quad \delta' = \frac{2\,\Delta\sigma_p\, t(1 - R)(1 + 1/N)(1 + h/(1 - x^2))}{3E} K_b. \qquad \text{Eq. 23}$$

Pillar Formula for Shallow Workings. The net closure at the pillar, $2\,\Delta\delta_p$, will be the algebraic sum of all the effects described above plus the abutment deflection which, as the stress concentration will be the same in the top and bottom of the abutment, must be effectively equal to δ_A of Equation 10(b):

$$2\,\Delta\delta_p = (\delta - \delta_r + \delta_A - \delta' - \delta'_p)_{roof} + (\delta - \delta_r - \delta' - \delta'_p)_{floor}$$

$$\frac{2\,\Delta P h'}{A_p E_p} = \left[\frac{S_o R\, t\, K_b}{E} - \mu_p \frac{S_t h'}{E_p} + \frac{(2 S_o R - S_t h(1 - \mu))h'}{E} - \frac{2\,\Delta\sigma_p\, t(1 - R)(1 + 1/N)(1 + h/(1 - x^2))\,K_b}{3E} - \Delta\sigma_p \frac{R B(1 - \mu)}{\pi E}\right]_{roof}$$

$$+\left[\frac{(2 S_o R - S_t h(1 - \mu)(\sqrt{1 - x^2} + h)}{E} - \mu_p \frac{S_t h'}{E_p} - \frac{\pi\,\Delta\sigma_p\, t(1 - R)(1 + 1/N)(1 + h/\sqrt{1 - x^2})}{2E} - \frac{\Delta\sigma_p R B(1 - \mu)}{\pi E}\right]_{floor}$$

Converting to plane strain and simplifying as for Equation 15:

$$\frac{\Delta\sigma_p}{S_o} = \frac{(2R - kh(1-w))(\sqrt{1-x^2} + 2h) + RK_b' - 2w_p khn}{2hn + (\pi/2(1+h/\sqrt{1-x^2}) + 2K_b'/3(1+h/(1-x^2))(1-R)(1+1/N) + 4bR(1-w)/\pi}$$

Eq. 24

and

$$\frac{\sigma_p}{S_o} = \frac{\Delta\sigma_p}{S_o} + 1 \qquad \text{Eq. 15(c)}$$

where all symbols are as defined for Equation 15 except K_b' in plane strain:

$$K_b' = \frac{1-x^2}{2z'^3} + \frac{1.2(1+w)(1-x^2)}{z'} + \left[13 - 2w\left\{\frac{12(1-x'^2)}{z'^2} + 1 - \frac{8}{z'^2} - 3w\right\}\right]\frac{z'}{32} + \frac{0.884F(1-x'^2)}{z'^2}$$

and

$$F = 1 - \frac{1}{2.26/z' + 1}, \quad z' = z/t.$$

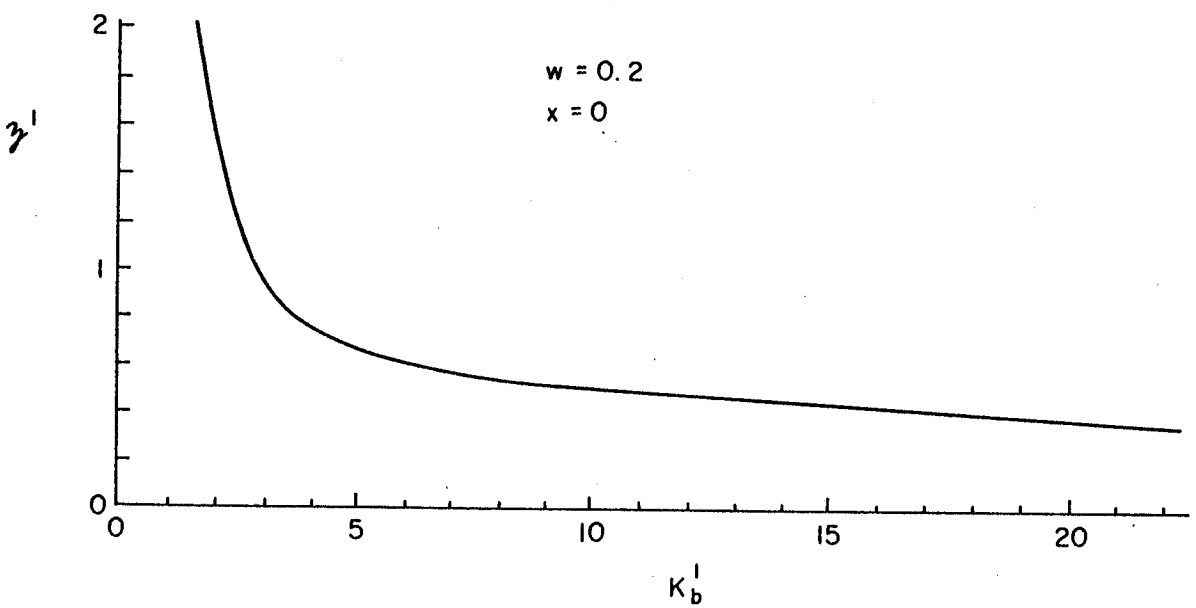

Figure 17. Variation of K_b' with z'

Comparison of Shallow Case with Deep Case. The preceding analysis for shallow mining zones should be more valid for shallow mining zones than for deep zones. From theoretical considerations of stress distribution, the depth of cover required for the deep analysis would be quite large; however, with the acceptable tolerances on such equations when used in practice, the appropriate ranges for each of these analyses may not be entirely governed by such theoretical considerations. Also, some evidence is provided by knowing that when the depth of a beam becomes greater than its span the conventional beam analyses start to give significant errors.

In Figure 18 a typical set of parameters describing a mining zone is used to compare the change in pillar stresses with changes in depth-to-span ratio as predicted by the tributary area theory with the corresponding changes predicted by the proposed hypothesis for deep and shallow mining zones. These curves suggest that in the centre of the mining zone the hypothesis for the shallow case should be used for values of z/L less than 1.

From a practical point of view, it would probably be reasonable to limit the use of the rather elaborate equation for the shallow case to values of z/L greater than 0.5, as the curves in Figure 18 suggest that for lower ratios the tributary area theory would provide a lower and possibly more valid answer. On the other hand, the reason for the hypothesis predicting pillar loads greater than those predicted by the tributary area theory is the fact that the shape of the deflection curve of the roof will increase the load on the central pillars to values greater than the average and hence greater than the load of the tributary area surrounding them.

Alternatives to the Elastic Analysis

Yielding Wall Rock with Horizontal Workings. Whenever elastic theory is used for a problem in rock mechanics, the question is raised regarding the applicability of this theory to a medium which for many reasons may not behave like a perfectly elastic, homogeneous, isotropic body. However, aside from the fact that there is no other theory that is as serviceable for a deformable medium, use of the elastic theory has some justification. Many rocks produce straight line stress-strain curves, particularly on the loading cycle and more particularly for increments of stress, which satisfies the principal requirement of elasticity for determining the effects of increased loadings.

Furthermore, any other ground reactions to stress, e.g., visco-elastic, plasto-elastic, elasto-plastic, etc., can be considered as modifications of the answer obtained from the elastic solution. The solutions for these other materials, if they could be obtained, would still include the same equilibrium equations and boundary conditions as used

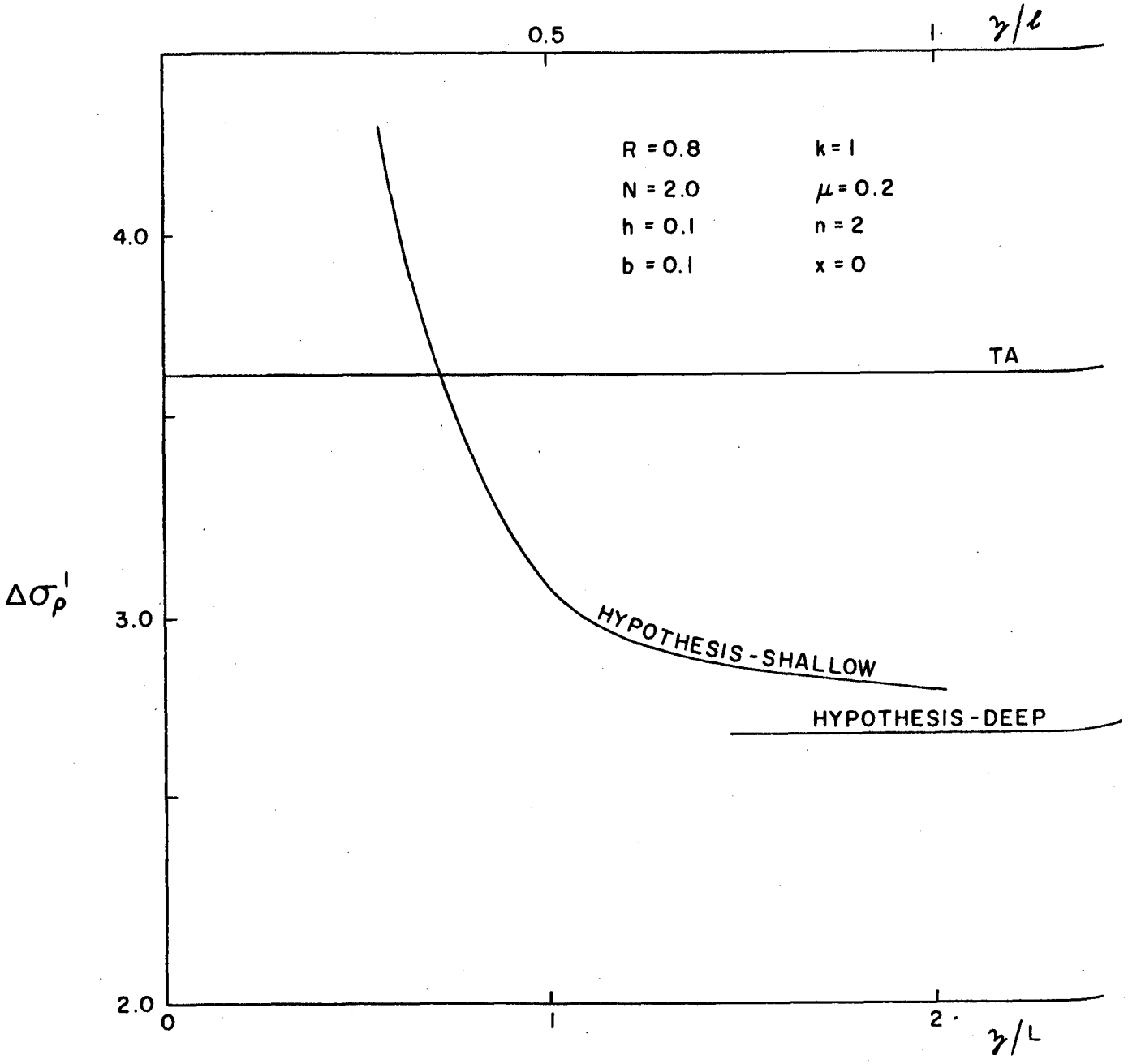

Figure 18. Comparison of Pillar Loading Theories

in the elastic analysis. Only the compatibility equation would be different. Hence the elastic solution can always be considered as a first approximation.

An analysis of pillar loadings is made below, assuming that the roof over horizontal workings will behave like a yielding mass, in the sense that a granular mass will yield without a complete breakdown of its strength. The compatibility equations of elastic strain can be replaced by the stress relations at a point when yielding occurs. Then the implications with respect to pillar loading of the deformation requirements to fulfil the yielding condition are examined.

If the ground over the workings does not act like an elastic mass, it is possible that some yielding could occur with the stress distribution being governed by the Mohr strength parameters rather than by compatible elastic strains (12). If yielding occurs along vertical planes as shown in Figure 19, the following derivation can be used: A horizontal slice dz will be acted upon by σ_v on the top surface, σ_v and $\partial\sigma_v$ on the bottom surface, τ and σ_h on the sides, and ∂W as a body force, hence:

$$\Sigma F_v = \partial W + 2\iota\sigma_v - 2\iota(\sigma_v + d\sigma_v) - 2\tau\, dz = 0$$

as $$\partial W = 2\gamma\, \iota\, dz$$

$$\frac{d\sigma_v}{dz} = \gamma - \tau/\iota.$$

With incipient yielding along the vertical planes on which τ is acting, the maximum value of τ is governed by the strength parameters of the ground according to Mohr's strength theory:

$$\tau = c + \sigma_h \tan \phi$$

where c is the cohesion or shear strength at zero normal stress and ϕ is the angle of internal friction. σ_h can be related to σ_v by assuming a constant coefficient of lateral pressure, k, so that $\sigma_h/\sigma_v = k$.

$$\therefore \frac{d\sigma_v}{dz} = \gamma - c/\iota - k\sigma_v \tan \phi/\iota.$$

The solution of this differential equation gives (74):

$$\sigma_v = \frac{\gamma\iota - c}{k \tan \phi} \left(1 - e^{-kz \tan \phi/\iota}\right)$$

and for pillars $\sigma_v = S_p$.

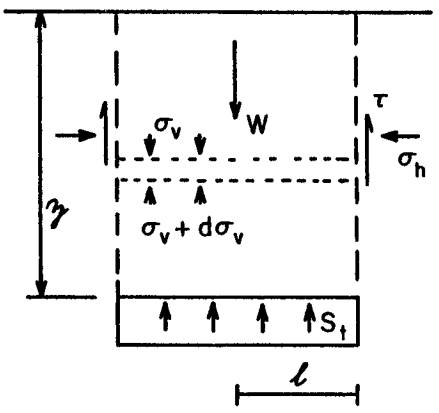

Figure 19. Stresses in Yielding Ground Over an Opening

From Figure 20 it can be seen that there is a necessary relationship between σ_h and σ_v. Thus:

$$k = \sigma_h/\sigma_v$$

$$= \frac{\sigma_v - 2c \tan \phi}{\sigma_v(1 + 2 \tan^2 \phi)} .$$

From this equation it follows that for $\phi = 45^o$ when $c = \sigma_v/2$, $k = 0$, and when $c \longrightarrow 0$, $k \longrightarrow 0.333$. These figures indicate the possible range for k which is different from the arbitrary value of 1 recommended previously based on an erroneous deduction from experiments (74).

One limiting case would be when $c \longrightarrow 0$; the pillar loading according to this theory would be for $k = 0.333$ and $\phi = 45^o$:

$$S_p \leq 3\gamma t (1 - e^{-0.333\, z/t})$$

and

$$\sigma_p \leq \frac{S_p}{1 - R} \leq \frac{3\gamma t}{1 - R} (1 - e^{-0.333\, z/t}). \qquad \text{Eq. 25}$$

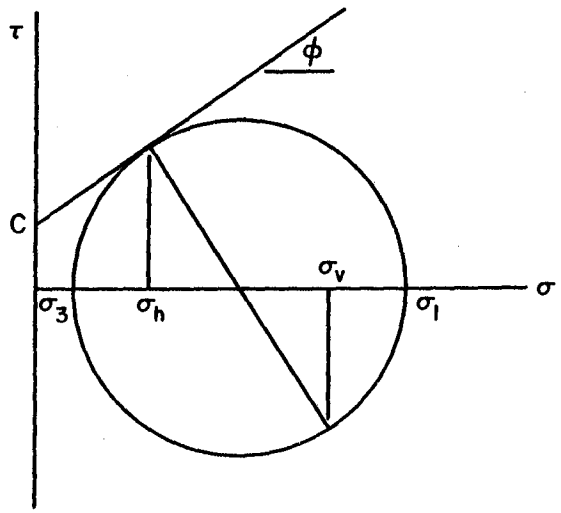

Figure 20. Mohr Circle of Stress for Abutment Zones

Figure 21 shows the effect of the ratio z/ℓ on the loading pressure, S_p, as included in Equation 25. As z/ℓ increases, the proportion of the total pressure, γz, that is applied to the pillars decreases so that it is less than 0.5 when $z/\ell > 5$ or the depth-to-span ratio is greater than 2.5. At the same time, the loading, S_p, as a function of the span increases with z/ℓ but at a decreasing rate and asymptotically to $3\gamma\ell$. Figure 21 is for the limiting case of $c = 0$.

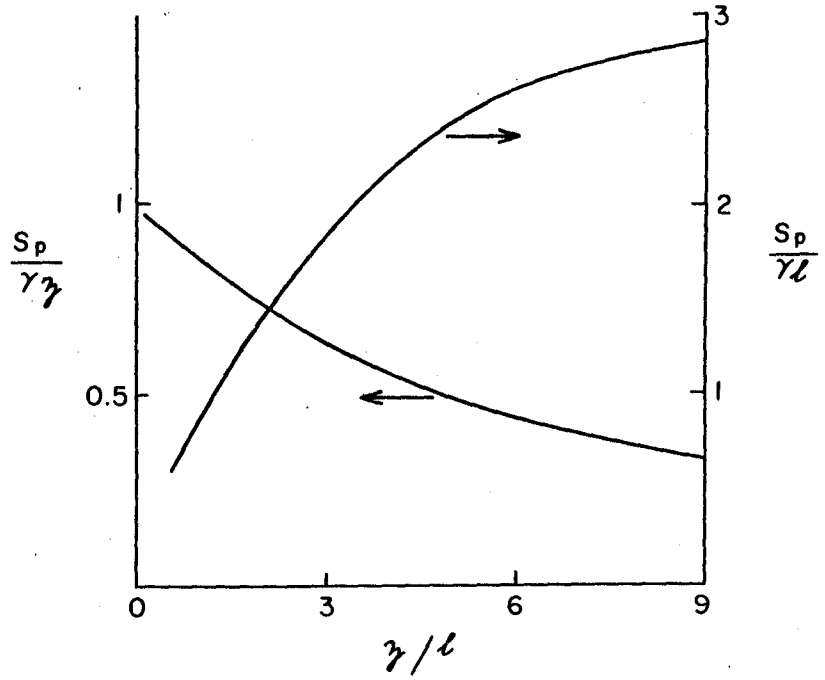

Figure 21. Variation of Average Pillar Pressure with Span of Mining Zone

It is difficult to compare Equation 25 with the elastic hypothesis represented by Equations 15 and 24, as there are many parameters that are not common. Therefore, a typical example will be used for comparison.

Example: $z = 3000$ ft, $\ell = 1000$ ft, $h = 0.01$, $b = 0.04$, $N = 10$,
$x = 0$, $\gamma = 170$ pcf, $\mu = 0.2 = \mu_p$, $E = 1 \times 10^6$ psi, $R = 0.5$.

For Yielding Wall Rock from Equation 25, $\sigma_p = 1.26\ \gamma z$.

For Elastic Hypothesis from Equation 15, $\sigma_p = 1.61\ \gamma z$.

Hence by the elastic analysis for this case, the pillar stress would be 28% greater than predicted by Equation 25. However, part of this difference results from Equation 15 including the variation of σ_p with x, and thus at $x = 0$ σ_p is greater than the average; whereas Equation 25 does not include this variation, nor can it do so without some new theory of plasticity. Hence Equation 25 provides an average figure. From Figure 21 it can be deduced that, at a depth three times greater than in the example (or for 1/3 of the span), Equation 25 would give $\sigma_p \simeq 0.65\ \gamma z$ with the elastic equation 15 giving a stress 248% greater.

However, the other serious criticism of Equation 25, aside from not including a function of x, is that the required strains or deformations to produce yielding are ignored. It is probable that such strains could not be produced except with very large pillar deformations. For example, experiments have shown that for granular material a yielding condition as represented by Equation 25 would require a vertical deformation at the bottom of the yielding mass of 0.035 of the span (71). For the above example:

$$\delta_v = 0.035 \times 2 \times 1000 = 70 \text{ ft},$$

which would require not only pillar deformation but also considerable extraction.

For solid rock, although no experiments have been conducted to obtain such data, it is probable that the vertical deformation required for yielding would be much less. If the in situ compressive yield stress were in the above example 1000 psi, then theoretically an estimate could be made by calculating the vertical deformation at this stress. This would be a minimum figure, as yielding would produce additional strain.

Recognizing that the major principal stress along the yielding surface is at $(45^\circ + \phi/2)$, or for ϕ of 45° at 67.5°, to the horizontal, it could follow that the vertical deformations at yielding would be:

$$\delta_r \geq \epsilon_f \cdot \frac{t}{\cos 67.5} \cos 22.5 \geq \epsilon_f t/\tan 22.5,$$

where ϵ_f is the compressive yield strain. For the example the yield strain would be at least 1000 μ, hence

$$\delta_v \geq \frac{1000}{10^6} \times 1000/\tan 22.5 \geq 2.4 \text{ ft.}$$

$$\therefore \quad \sigma_p \geq \frac{2.4 \times 10^6}{1000 \times 0.01 \times 2} \geq 120,000 \text{ psi,}$$

which would be impossible. As a result of this analysis, it seems that a yielding roof (in the sense described above) is not likely to occur with pillar support.

Arching from Bending over Horizontal Workings. Another concept that is often the subject of speculation is that a rock mass in situ is similar to uncemented masonry insofar as it is made up of a series of intimately interlocking blocks and cannot sustain tensile stresses. Following some previous work (72), the implications of the roof rock over a mining zone behaving like masonry are examined below. From a knowledge of the stress distribution around horizontal underground openings with the major principal field stress being vertical, it can be expected that there will be a tendency for tensile stresses to occur in the immediate roof rock near the centre of the mining zone. Also, as a result of the deflection of the ground surface over the workings, some tension might occur. This has actually been measured on many occasions at the ground surface over the abutment zones of the mining zone (83).

By analysing the implications of the ground not sustaining tensile stresses where these dilations occur, a modified stress distribution in the roof rock is obtained. The resultant loading on the pillar supports might then be considered to be either the dead weight of the detached rock within the dilated zone of the immediate roof or the result of the deformation of the roof resulting from the modified stress distribution. These two approaches, of course, should provide the same answer.

The assumptions in this theory are that the ground overlying the mining zone tends to bend like a beam but that no tensile stresses can exist (72). This results in tensile cracking adjacent to the ground surface over the abutments and at the centre of the roof. The resultant abutment and crown stress distributions are then as shown in Figure 22, which is typical of a masonry arch at ultimate load. It is also assumed that the depths of cracking at the abutments and crown are equal (hence nz in Figure 22 is common to the abutments and crown); that the maximum stresses, σ_m, are equal; and that the interlocking of the blocks of roof

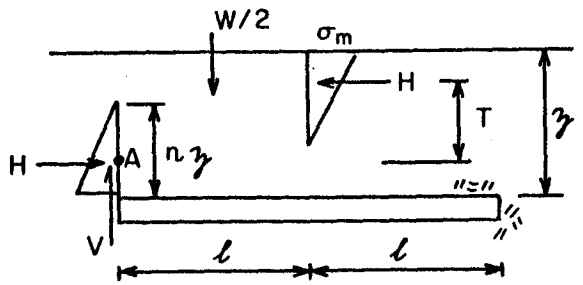

Figure 22. Arching-Bending Over Horizontal Workings

rock holds them in place. It then follows that:

$$\Sigma M_A = (W/2)(\ell/2) - HT = 0$$

i.e., the resisting moment $M = HT$

$$\therefore M = \frac{\sigma_m}{2} nz\left(z - \frac{2nz}{3}\right) = \frac{\sigma_m z^2 n}{2}(1 - 2n/3)$$

and

$$\partial M/\partial n = 1 - 4n/3 = 0$$

$$\therefore \quad n = 3/4.$$

This agrees with the results obtained in certain experiments on brick beams (72).

This theory was formulated to explain the mechanics of roof deformation (72). However, provided that σ_m is less than the compressive strength of the rock, it should follow that the ultimate pillar loading at $x = 0$ would be produced by the weight of loose rock, i.e.,

$$\sigma_p = \frac{0.25\,\gamma z}{1 - R}. \qquad \text{Eq. 26}$$

For the above example, Equation 26 would give $\sigma_p = 0.50\,\gamma z$. Paradoxically, the elastic hypothesis would predict a stress 322% greater.

Two serious criticisms can be made of this theory: bending action as postulated could not, as indicated by many experiments, validly represent cases where $z/\ell \gtrsim 2$. Secondly, the strain or deformation of the roof that would be associated with this action is likely to be

greater than can actually occur without unrealistic pillar deformations, as will be shown below.

The deformation of the roof in this case arises from two mechanisms: the bending stresses in the beam, and the axial compression along the line of thrust. The bending deformation is that of a semi-fixed beam. The deflection for a fixed beam at the centre is known to be

$$\delta_c' = \frac{w L^4}{384 E I}.$$

To change the beam as shown in Figure 23(a) with the bending moment diagram of Figure 23(b) to that postulated above, i.e., with equal maximum stresses at the crown as at the abutments, it is necessary to add the bending moment, $wL^2/48$, shown in Figure 23(c), to produce the required diagram shown in Figure 23(d). The additional deformation caused by this added moment can be determined by taking the moment of the area of the bending moment diagram between the abutment and the ℄ about the abutment. Thus, for the semi-fixed beam the total deflection is:

$$\delta_c'' = \frac{w L^4}{384 E I} + \frac{w L^2}{48} \frac{L}{2} \frac{L}{4 E I} = \frac{w L^4}{192 E I}$$

or

$$\delta_c'' = \frac{(\gamma)(0.75 z) L^4}{192 E (0.75z)^3/12} = \frac{\gamma L^4}{9 E z^2}.$$

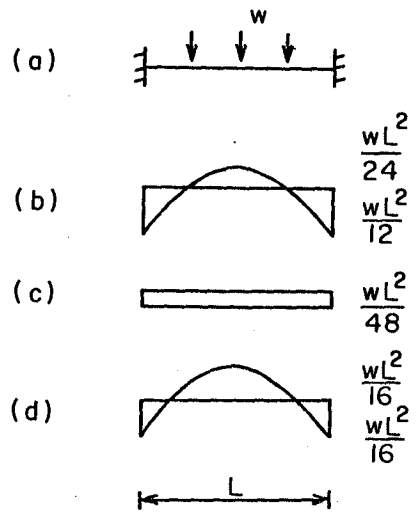

Figure 23. Bending Moment Diagrams for Arching-Bending

The deformation resulting from compression along the line of thrust can be obtained by assuming this line is parabolic with the length represented very closely by:

$$\lambda = L + \frac{8\,T^2}{3L}$$

or

$$T = \left\{\frac{3L}{8}\,(\lambda - L)\right\}^{\frac{1}{2}}$$

$$\frac{\partial T}{\partial \lambda} = \frac{3L}{16}\left\{\frac{8}{3L - 3L^2}\right\}^{\frac{1}{2}}$$

and

$$\partial \lambda = \lambda \epsilon_\lambda$$

where ϵ_λ is the average strain along the line of thrust (72). This average can be determined roughly (if it were an important quantity it would warrant a more rigorous analysis) by recognizing that at a point near the quarter span the moment in the beam will be zero, see Figure 23(d). With the thrust, H, being equal to that at the abutments or crown, it follows that

$$\frac{1}{2}\,\sigma_m \cdot \frac{3}{4}\,z = \sigma_{1/4}\,z$$

$$\therefore \sigma_{1/4} = \frac{3}{8}\,\sigma_m.$$

By taking a simple arithmetical average, the average stress is:

$$\sigma_{avg} = 7\sigma_m/16 = \frac{7H}{6z} = \frac{7}{24}\,\frac{\gamma L^2}{z}$$

$$\therefore \partial \lambda = \left\{L + \frac{8\,T^2}{3L}\right\}\frac{7\gamma L^2}{24\,z\,E} = (3L^2 + 2z^2)\,\frac{7\gamma L}{72\,z\,E}$$

$$\therefore \delta_c''' = \partial T = \frac{7\gamma L^2}{192E}\,(3(L/z)^2 + 2).$$

Now

$$\delta_c = \delta_c'' + \delta'''$$

$$= \frac{\gamma L^4}{9E\,z^2} + \frac{7\gamma L^2}{192\,E}\,(3(L/z)^2 + 2)$$

$$= \frac{\gamma L^4}{3z^2 E}\left\{\frac{127}{192} + \frac{7z^2}{32L^2}\right\} = \frac{\gamma\, t^4}{96\,z^2 E}\left\{\frac{127}{6} + \frac{7z^2}{t^2}\right\}.$$

A feasible example where this theory would be most applicable is: $z = 1000$ ft, $\ell = 1000$ ft, $h = 0.01$, $\gamma = 170$ pcf and $E = 5 \times 10^6$ psi. Hence

$$\delta_c = \frac{170 \times 1000^4}{96 \times 1000^2 \times 144 \times 5 \times 10^6} \left\{ \frac{127}{6} + 7 \times 3^2 \right\} = 0.207 \text{ ft.}$$

$$\therefore \sigma_p = \frac{0.207 \times 5 \times 10^6}{1000 \times 0.01 \times 2} = 52,000 \text{ psi,}$$

which would be impossible except for $R > 98\%$.

This theory also does not take into account the additional pillar deformation required for the detachment of the tensile zone nor does it include the factor k (i.e., S_t/S_o). These criticisms need not be amplified in view of the demonstrated inadequacy to account for compatible elastic strains.

In summary, the analysis shows that with pillar support, as opposed to yielding support, in most circumstances insufficient deformation could occur to permit the detachment and dead weight loading from the roof rock implied by this theory.

Doming over Horizontal Workings. An alternate analysis has been made, based on the same concept of a rock mass behaving like uncemented masonry (4). In this case, it is postulated that a dome of detached rock develops over mine workings. Whereas the theory was not postulated for the determination of pillar loading, the implication must follow that the pillars would be loaded with the weight of the detached rock within the dome.

An attempt was made to predict quantitatively the height of the dome that forms over a mining zone such that the rock within the dome separates from the dome boundary (4). As such it is an alternative to the Arch-Bending theory examined above.

It is stated that the "vertical downward load F_v at a point on the dome boundary of x" is (4):

$$F_v(x) = \int_o^x \gamma z \, dx = \gamma z x$$

But if a dome actually exists this seems to ignore the diffraction of gravitational stress around the dome to produce a concentration of σ_t in the sides.

However, the theory produces an answer that seems to be not unreasonable. However, it will be shown below that for detachment of the core of the dome incompatible strains would be required. To establish this point the other parts of the theory will be explained.

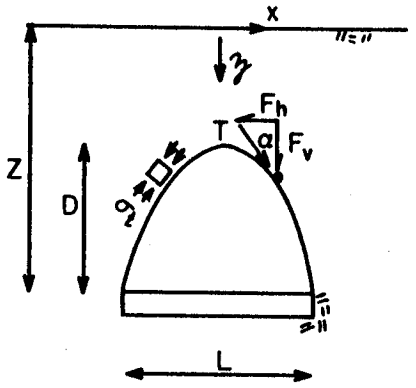

Figure 24. Doming Over Horizontal Workings

The assumption is then made that the shape of the dome develops so that the horizontal force component, F_h, nowhere exceeds a critical value S (4). It is implicitly assumed that, for creation of the dome, $F_h = S$ at all points.

$$\therefore\ S = \gamma z x\, dx/dz.$$

Integrating:

$$S \ln z = \gamma x^2/2 + K.$$

For the boundary condition $x = L/2$ and $z = Z$ it follows that:

$$K = S \ln Z - \gamma L^2/8$$

$$\therefore\ z = Z e^{\gamma(x^2 - L^2/4)/2S}.$$

If $z = Z - D$, where D is the height of the dome,

$$L^2 = \frac{8S}{\gamma} \ln \frac{Z}{Z - D}.$$

Then the assumption is made that S cannot be greater than $Q_u (Z - D)$ where Q_u is the uniaxial compressive strength of the rock mass above the dome. Thus

$$L = \left\{ \frac{8 Q_u Z}{\gamma} (D/Z - 1) \ln (1 - D/Z) \right\}^{\frac{1}{2}}.$$

From $d_L/d_D = 0$, the largest span and height of dome are obtained:

$$D_{max} = \frac{e - 1}{e} Z = 0.63 Z$$

$$\therefore \sigma_p = \frac{0.63 \gamma Z}{1 - R} \text{ for } x = 0.$$

For the example, $\sigma_p = 1.26 \gamma z$ whereas the elastic hypothesis gives $1.61 \gamma z$ or 28% greater stress. Similarly to the Arch-Bending theory, the Doming theory ignores many undoubtedly significant parameters such as k (i.e., S_t/S_o), and n (i.e., E/E_p).

The main question for this theory, as for the two preceding theories, is whether the strains or deformations are compatible with the load calculations. The Arch-Bending theory showed that the deformation of the solid ground was too great to be accommodated by the pillars. In the Doming theory another aspect can be examined. If there is detachment of rock from the dome, the detached rock must expand, and this expansion must be consistent with the load calculations. The deformation required for detachment at x = 0 is:

$$\delta = \int_{0.37 Z}^{Z} \frac{\gamma z}{E} dz = 0.432 \gamma Z^2/E.$$

As this deformation must be in addition to the deformation that exists in the undisturbed ground, it is a measure of the increase in stress.

$$\therefore \Delta\sigma_p = 0.432 \gamma Z^2/E \div h'/E_p = \frac{0.432 \gamma Z^2}{n h'}.$$

For the above example this gives

$$\Delta\sigma_p = 0.432 \times 170 \times 3000^2/(2 \times 10) = 230,000 \text{ psi},$$

which is impossible; hence detachment cannot occur without considerable deformation equivalent to about 5 feet.

Summarizing, it can again be seen that the deformation necessarily associated with the development of a detached zone, which might be the loading on pillars, is excessive and incompatible with the relatively rigid nature of pillar support.

Elliptical Arching. In view of the inadequacies of the theories that have been postulated to describe the consequences of a rock mass acting like uncemented masonry (4, 72), a more satisfactory theory of loading through detachment is now postulated. The theory suggested below overcomes the limitations inherent in the previous theories of being only applicable to horizontal workings and of implicitly assuming that the horizontal field stress is zero.

With the knowledge that has been established on the boundary stresses around elliptical openings (73), it is possible to calculate the minimum rise of an elliptical arch that would eliminate tension in the centre of the roof or wall rock for any depth and for any combination of major and minor principal field stresses. If any doming occurs over mine workings, this theory is likely to provide a more accurate prediction of the extent of such doming.

The following assumptions are made in developing this new theory:

1. No tension can exist in the walls.
2. An elliptical arch will occur with an axial ratio just sufficient to eliminate tension from the arch.
3. Pillar loads occur from the detachment of the rock within the elliptical arch.

The equation for the boundary stress, σ_n, around an ellipse in plane stress is (73):

$$\frac{\sigma_n}{S_o} = \frac{2v(1+k)+(1-k)\{(1-v^2)\cos 2\beta+(1+v^2)\cos 2(\beta-n)\}}{(1+v^2)+(1-v^2)\cos 2n}$$

where $v = a/b$, $k = S_t/S_o$, β = angle clockwise from the major axis to the x-axis, and n = elliptic coordinate clockwise from the major axis.

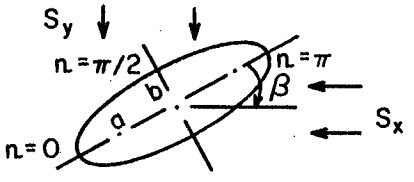

Figure 25. Elliptical Hole in Biaxial Stress Field

For the case where the field stresses are parallel and normal to the seam, then the height of arch can be obtained for no tension by letting $\beta = 0$, $n = \pi/2$, and $\sigma_n = 0$.

$$\therefore \; v = 2k/(1-k)$$

$$\text{or} \quad c/\ell = (1-k)/2k.$$

There will be limits on this equation such that $0 < k < 1$; in other words, if $k = 0$ tension cannot be eliminated at the crown and if $k = 1$ there can be no tension even in a flat back, i.e., $c = 0$.

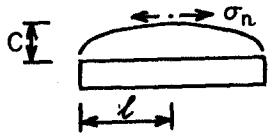

Figure 26. Elliptical Arching Over Horizontal Workings

The boundary of the ellipse can be represented by the equation:

$$\frac{x^2}{a^2} + \frac{y^2}{b^2} = 1$$

$$\text{or} \quad y = (1 - x^2/a^2)^{\frac{1}{2}}\, b.$$

Hence, a pillar stress equation could be set up as follows:

$$\sigma_p = \frac{\gamma c}{1-R} = \frac{\gamma \ell}{2k} \frac{1-k}{1-R} (1-x^2)^{\frac{1}{2}}$$

where $x = x'/\ell$. This equation would apply to horizontal workings.

For a vertical seam a bin-type pressure, calculated using the above theory for Yielding Wall Rock, could be used for determining the horizontal stress, S_i, in the detached rock:

$$S_i = \gamma c (1 - e^{-z/c}).$$

For $z/c \gtrsim 3$, $S_i = \gamma c$; hence the case of the vertical seam produces the same pillar stress equation as for the horizontal seam. It should be repeated, however, that this equation could only be valid where considerable deformation is possible. The actual amount required could be calculated

for any given conditions. However, these alternatives are obviously inferior to the elastic hypothesis formulated herein, for the reasons analysed above. Even for unusual wall rocks or pillars this is likely also to be true.

Consequently, the conclusion is reached that except in very unusual cases, elastic theory will be the most valid theory for the determination of stress and deformation around mining openings.

ACKNOWLEDGEMENTS

During this work Mr. N. Toews, of the Physics Section of this Division, has provided invaluable guidance as well as original work on the solution of the deflection of an elliptical hole. Miss M. Ellis has provided valuable assistance in compiling the manuscript. The editing was done with the good services of Mr. P.E. Shannon of Mines Branch.

- - - -

DFC:DV

BIBLIOGRAPHY

1. Morrison, R.G.K., lecture notes (1963).

2. Merrill, R. et al., "Stress Determinations by Flatjack and Borehole-Deformation Methods", USBM RI 6400 (1964).

3. Morrison, R.G.K. and Coates, D.F., "Soil Mechanics Applied to Rock Failure in Mines", Bull. CIMM, Vol. 48, No. 523 (1955).

4. Denkhaus, H., "Critical Review of Strata Movement Theories and Their Application to Practical Problems", J. South African IMM (March, 1964).

5. Freidman, M., "Petrofabrics", Internat. Conf. State of Stress in the Earth's Crust - preprint of papers; Rand Corp., Santa Monica, RM-3583 (1963).

6. Duvall, W., "Stress Analysis Applied to Underground Mining Problems, Part II. Stress Analysis Applied to Multiple Openings and Pillars", USBM RI 4387 (1948).

7. Denkhaus, H., "A Critical Review of the Present State of Scientific Knowledge Related to the Strength of Mine Pillars", J. South African IMM, Vol. 63, No. 2, p. 59 (September, 1962).

8. Alder, H. et al., "Research on Strata Control in the Northern Coal Field of Great Britain", Internat. Conf. about Rock Press. and Support in the Workings, p. 106, Liege (1951).

9. Steart, F., "Strength and Stability of Pillars in Coal Mines", J. Chem. Met. and Min. Soc. of South Africa (March, 1954).

10. Avershin, S., "Experiences in Rock Pressure Research", Internat. Strata Control Congress, Leipzig (1958).

11. Tincelin, E. and Sinou, P., "Collapse of Areas Worked by the Small Pillar Method - Practical Conclusions and an Attempt to Formulate Laws for the Phenomena Observed", Internat. Conf. on Strata Control, Paris, p. 571 (1960).

12. Coates, D.F., "Theoretical Consideration of the Effect of the Ratio of the Width of Mine Area to Depth of Operations in Pillar Loading - Elastic and Plastic Analyses", Appendix D in Report of the Special Committee on Mining Practices at Elliot Lake, Part II; Ontario Dept. Mines, Bull. 155 (1961).

13. Gimm, V., "Rock Mechanical Observations During Pillar Extractions in Bleicherode, and Conclusions Resulting from the Extraction Work in Potash Mining", New Hutte, 6 Jg, Heft 1 (1961).

14. Avershin, S., "Room Pillar", Technical Digest, Prague, Statno Naklo Tek Literature (Oct. 1961).

15. Storck, U., "Recent Findings of Ground Stress Research as Applicable to Potassium Mining Practices", Bergbauwissenschaften, Vol. 9, 15/16, p. 341 (1962).

16. Hofer, K. and Menzel, W., "Comparative Study of Pillar Loads in Potash Mines Established by Calculation and by Measurements Below Ground", Internat. J. Rock Mech. and Mining Sci., Vol. 1, p. 181 (1964).

17. Trumbachev, V. and Melnikov, E., "Distribution of Stress in Inter-room Pillars and the Immediate Roof", Gosgortekhizdat, Moscow (1961).

18. Panek, L., "Stresses About Mining Openings in a Homogeneous Rock Body", Edwards Bros Inc., Ann Arbor, Michigan (1951).

19. Hiramatsu, Y. and Oka, Y., "Photoelastic Investigations into the Earth Pressure Acting on Pillars", J. MM Japan, Vol. 79, No. 905 (1963).

20. Chih-Bing Ling, "On the Stresses in a Plate Containing Two Circular Holes", J. Applied Physics, Vol. 19, p. 77 (1948).

21. Schoulz, K., "Over Den Spannungstoestend in Doorborde Platen", Diss Techn Hochschule, Delft (1941).

22. Hutter, A., "Die Spannungsspitzen in Gelochten Blechscheiden Und Stereifen", Z. Ange Math. Mech., Vol. 22, p. 322 (1942).

23. Potts, E., Discussion of "Some Problems of Strata Control and Support in Pillar Workings" by Bryan, A. et al., Mining Engineer, Vol. 123, No. 41, p. 238 (1964).

24. Buchanan, J.G., "The Load Cell Installation in No. 3 Mine, Dominion Wabana Ore Limited, Bell Island, Newfoundland", unpublished report, Mines Branch, Ottawa (1955).

25. Mohr, H., "Measurement of Rock Pressure", Mine and Quarry Engineering (May, 1956).

26. Leeman, E. and van Heerden, W., "Stress Measurements in Coal Pillars", Colliery Engineering (Jan. 1964).

27. Trumbachev, V. and Melnikov, E., "Distribution of Stresses in the Intervening Pillars at Medium and Steep Dips", Proc., Internat. Conf. on Strata Control and Rock Mech., Columbia Univ., New York (1964).

28. Obert, L., "Measurement of Pressures on Rock Pillars in Underground Mines, Part II", USBM RI 3521 (1940).

29. Obert, L., "Measurement of Pressures on Rock Pillars in Underground Mines, Part I", USBM RI 3444 (1939).

30. Hast, N., "The Measurement of Rock Pressure in Mines", Sveriges Geologiska Undersokning, Arsbok 52, No. 3, Stockholm (1958).

31. Naugchi, I. et al., "Measurement of Stress in Pillars at Kamioka Mine", J. MMI Japan, Vol. 75, No. 849 (1959).

32. Westergaard, H., "Bearing Pressures and Crack ", Trans. ASME, Vol. 61, A-49 (1939).

33. Hackett, P., "An Elastic Analysis of Rock Movements Caused by Mining", Trans. Inst. of Min. Eng., Vol. 118, Part 7 (April, 1959).

34. King, H. and Whetton, J., "Mechanics of Mine Subsidence", Congress on Ground Movement, Univ. of Leeds (1957).

35. Berry, D., "An Elastic Treatment of Ground Movement Due to Mining - I. Isotropic Ground", J. Mech. Phys. Solids, Vol. 8, p. 280 (1960).

36. Berry, D. and Sales, T., "An Elastic Treatment of Ground Movement Due to Mining - II. Transversely Isotropic Ground", J. Mech. Phys. Solids, Vol. 9 (1961).

37. Berry, D. and Sales, T., "An Elastic Treatment of Ground Due to Mining - III. Three Dimensional Problem, Transversely Isotropic Ground", J. Mech. Phys. Solids, Vol. 10 (1962).

38. Orchard, R., "Surface Effects of Mining - The Main Factors", Trans. Inst. Min. Eng., Vol. 116, p. 941 (1956-57).

39. Barcza, M. and Von Willich, G., "Strata Movement Measurements at Harmony Gold Mine", Assoc. Mine Managers South Africa, Paper No. 7 (1958).

40. Reed, J., "Case History in Pillar Recovery", Min. Eng., Vol. II, p. 701 (July, 1959).

41. Wardell, K., "The Problems of Analyzing and Interpreting Observed Ground Movement", Colliery Eng., Vol. 36, p. 529 (1959).

42. Wiggill, R., "The Effects of Different Support Methods on Strata Behaviour Around Stoping Excavations", J. South African IMM (April, 1963).

43. Muskelishvili, N., "Some Basic Problems of the Mathematical Theory of Elasticity", Noordhof, p. 216 (1951).

44. Salamon, M., "Elastic Analysis of Displacements and Stresses Induced by the Mining of Seam or Reef Deposits, Parts 1-4", J. South African IMM, Vol. 64, No. 4 (1963); Vol. 64, No. 6 (1964).

45. Ryder, J. and Officer, N., "An Elastic Analysis of Strata Movement Observed in the Vicinity of Inclined Excavations", J. South African IMM, Vol. 64, No. 6, p. 219 (1964).

46. Dischinger, F., "Contribution to the Theory of Wall-Like Girders", Internat. Assoc. for Bridge and Structural Eng., Zurich Publication, Vol. 1 (1932).

47. Chow, L. et al., "Stresses in Deep Beams", Proc. ASCE, Vol. 78, No. 127 (1952).

48. Saad, S. and Hendry, A., "Stresses in a Deep Beam with a Central Concentrated Load", SESA, Vol. 18, No. 1 (1961).

49. Saad, S. and Hendry, A., "Gravitational Stresses in Deep Beams", The Structural Engineer, Vol. 39, No. 6 (1961).

50. Lehr, E., "Modellversuche an Balken auf Elastischer Unterlage Zur Karung des Spannungsverteilung im Hangenden von Abbanortern", Erzbergbau Einschl. Aufbereitung, XXXII (N.F. XXIII), Jahrg., Heft 23 (1935).

51. O'Donnell, W., "The Additional Deflection of a Cantilever Due to the Elasticity of the Support", J. App. Mech. (Sept. 1960).

52. Coker, E. and Filon, L., "A Treatise on Photoelasticity", Cambridge University Press, p. 473 (1957).

53. Rosenhaupt, S., "Experimental Study of Masonry Walls on Beams", Proc. ASCE, Vol. 83, No. 3 (1962).

54. Terzaghi, K., "The Actual Factor of Safety in Foundations". The Structural Engineer, Vol. 13, p. 126 (1935).

55. Monfore, G., "Laboratory Tests of Rock Cores from the Foundation of Dam BR-9, India, and Analysis of Load Bearing Tests", USBR, Denver, Unpublished Laboratory Report No. C-731 (1954).

56. Belin, R., "Observations on the Behaviour of Rock When Subjected to Plate Bearing Loads", Australian J. of Applied Science, Vol. 10, No. 4, p. 308 (1959).

57. Habib, M., "Determination of the Moduli of Elasticity of Rocks In Situ", Inst. Tech. Bat. Trav. Pub. Ann., No. 145, p. 27 (1950).

58. Dvorak, A. and Peter, P., "Field Tests on Soils and Rocks", Proc. of 5th Internat. Conf. Soil Mech. and Foundation Engineering, Paris, Vol. 1, p. 453 (1961).

59. Serafim, J., "Rock Mechanics Considerations in the Design of Concrete Dams", Internat. Conf. on State of Stress in the Earth's Crust - preprint of papers; Rand Corp., Santa Monica, California, RM-3583 (1963).

60. Trumbachev, V.F., "The Effect of the Dip Angle of a Deposit on the Distribution of Stresses in Interchamber Pillars", Teknologia i E Konomika Ugleboychi, No. 3, Moscow (1962).

61. Merrill, R. and Peterson, J., "Deformation of a Bore Hole in Rock", USBM RI 5881 (1961).

62. Toews, N., personal notes (1964).

63. Timoshenko, S. and Goodier, J., "Theory of Elasticity, McGraw-Hill (1951).

64. Roark, R., "Formulas for Stress and Strain", McGraw-Hill (1954).

65. Bruggeman, J. et al., "Stresses and Pore Pressures Around Circular Openings Near a Boundary", USBR Tech. Memo 597, Denver (1940).

66. Caudle, R. and Clark, G., "Stresses Around Mine Openings in Some Simple Geological Structures", Univ. Illinois Engineering Experiment Station Bull. No. 430 (1955).

67. Hiramatsu, Y., Univ. of Kyoto, letter (1964).

68. Filon, L., "On the Elastic Equilibrium of Circular Cylinders under Certain Practical Systems of Load", Phil. Trans. Series A, Vol. 198, p. 147 (1902).

69. Pickett, G., "Application of the Fourier Method to the Solution of Certain Boundary Problems in the Theory of Elasticity", J. App. Mech., A 176 (1957).

70. Coker, E. and Filon, L., "A Treatise on Photoelasticity", Cambridge Univ. Press, p. 585 (1957).

71. Jahns, H. and Brauner, G., "Storage Pressure in Steep Measures", Internat. Conf. on Strata Control, Cherchar, Paris (1960).

72. Evans, W., "The Strength of Undermined Strata", Trans. IMM, Vol. L, p. 475 (1941).

73. Geldart, L. and Udd, J., "Boundary Stresses Around an Elliptical Opening in an Infinite Solid", Proceedings Rock Mech. Symp., McGill Univ.; Mines Branch, Ottawa (1963).

74. Terzaghi, K., "Theoretical Soil Mechanics", Wiley (1943).

75. Sneddon, I., "Stress in the Neighbourhood of a Crack", Proc. Royal Soc., Series A, Vol. 187, p. 229 (1946).

76. Dare, W., "Measuring Changes in Pillar Strain During Pillar Recovery", USBM RI 6056 (1962).

77. Nair, O. and Udd, J., "Stresses Around Openings in a Plate Due to Biaxial Loads Through a Superpositioning Technique", Proc. Rock Mech. Symp., Univ. of Toronto; Mines Branch (1965).

78. Ilstein, A., "The Problem of Applying Room System of Mining With Periodical Succession in the Distribution of Barrier and Inter-chamber Pillars", Symp. Methods for the Determination of Dimensions of Support Pillars and Arch Pillars, Academy of Sciences, Moscow (1962).

APPENDIX

GLOSSARY OF ABBREVIATIONS

(Note: After many of the terms, letters in brackets indicate the fundamental dimensions of the physical quantity; e.g., L stands for length, M for mass, F for force, T for time, and D signifies that the quantity is dimensionless.)

$a(L)$ - radius of a circle or major semi-axis of an ellipse

$A_o(L^2)$ - total area of walls adjacent to the mined out rooms or stopes of the entire mining zone

$A_p(L^2)$ - area of a pillar parallel to the walls

$A_t(L^2)$ - area of walls tributary to a pillar

$A_T(L^2)$ - area of walls adjacent to the entire mining zone

$b(D)$ - width of pillar (B/L)

$b(L)$ - minor semi-axis of an ellipse

$b_o(D)$ - width of opening (B_o/L)

$B(L)$ - width of pillar

$B_o(L)$ - width of opening (stope or room)

c c(L) - centre to centre

$cc(L^3)$ - cubic centimetre

$cf(L^3)$ - cubic foot

$c(FL^{-2})$ - cohesion

$ci(L^3)$ - cubic inch

$cm(L)$ - centimetre

cpn - compression

$C_b(D)$ - coefficient of $\frac{WL^3}{EI}$ for calculating the deflection of a beam due to bending moment

$C_s(D)$ - coefficient of $\frac{WL^3}{EI}$ for calculating the deflection of a beam due to shear force

$d(D)$ - parameter of an ellipse $(3 - 4\mu)$ in plane strain and $(3 - \mu)/(1 + \mu)$ in plane stress

$dia(L)$ - diameter

Eq. - equation

$E(FL^{-2})$ - modulus of linear deformation (Young's modulus)

$E_p (FL^{-2})$ - modulus of deformation of pillar rock

ft(L) - feet

F_s(D) - factor of safety

G (FL^{-2}) - modulus of shear deformation

h' (L) - semi-height of a pillar

h (D) - dimensionless height of a pillar (H /L)

H (L) - height of pillar

i (D) - angle of dip to horizontal

in. (L) - inch

I $(L^4$ or $ML^2)$ - moment of inertia

k (D) - S_t/S_o or σ_h/σ_v

k_s (L^3F^{-1}) - coefficient of subgrade reaction, δ/q

ksc - kilograms per square centimetre

l - semi-span of a mining zone (L/2)

ln a - natural logarithm of a

log a - logarithm of a to base 10

LF - linear foot

L (L) - breadth of mining zone

max - maximum

m (D) - Poisson's number

m (D) - parameter of an ellipse (a-b)/(a+b)

min - minimum

M (FL^{-2}) - $E/(1-\mu^2)$

M (FL)	- moment
n (D)	- ratio of moduli of deformation (M/Mp or E/Ep)
N (D)	- number of pillars
p (FL^{-2})	- contact pressure
pcf (FL^{-3})	- pounds per cubic foot
psf (FL^{-2})	- pounds per square foot
psi (FL^{-2})	- pounds per square inch
P (F)	- a pillar load
q (FL^{-2})	- bearing pressure
Q_B (FL^{-2})	- uniaxial compressive strength of a sample of width B
Q_o (FL^{-2})	- uniaxial compressive strength for a sample of unit width
Q_u (FL^{-2})	- uniaxial compressive strength
r (D)	- local extraction ratio, i.e. based on tributary area to single pillar
r (L)	- radius or radial distance
R (D)	- extraction ratio (wall area excavated/total wall area); parameter of an ellipse (a+b)/2
R (L)	- radius or radial distance
sf (L^2)	- square foot
si (L^2)	- square inch
S (L^{-3})	- section modulus
S_h (FL^{-2})	- field stress in the horizontal direction
S_t (FL^{-2})	- field stress parallel to the seam or vein and normal to strike
S_v (FL^{-2})	- field stress in the vertical direction

S_o (FL^{-2}) - field stress normal to seam or vein

S_p (FL^{-2}) - average pillar pressure on walls $\Sigma P/\Sigma A_t$

S_x (FL^{-2}) - field stress in the x-direction

S_y (FL^{-2}) - field stress in the y-direction

S_z (FL^{-2}) - field stress in the z-direction

tsn - tension

TA - tributary area

v_r (L) - radial displacement

v_θ (L) - tangential displacement

V (F) - shear force

w (D) - $\mu/(1-\mu)$

wrt - with respect to

W (F or MLT^{-2}) - load or weight

x (L or D) - linear displacement or co-ordinate or dimensionless distance (x'/L) in direction of x-axis

x' (L) - linear displacement or co-ordinate in direction of x-axis

y (L) - linear displacement or co-ordinate in direction of y-axis

z' (L) - dimensionless co-ordinate (z/L) in direction of z-axis

z (L or D) - linear displacement or co-ordinate in direction of z-axis

δ (L) - inward displacement of wall normal to vein or seam; or just displacement

δ' (L) - reverse displacement of wall due to average pillar pressure

δA (L) - abutment compression or deformation

$\delta_c(L)$ - displacement of wall normal to vein or seam at centreline

$\delta_e(L)$ - inward displacement of wall normal to vein (or seam), resulting from excavation of stopes or rooms

$\delta'_p(L)$ - local penetration of a pillar into the wall

$\delta_x(L)$ - displacement of wall normal to vein or seam at x from centreline

$\gamma(d)$ - shear strain

$\gamma(FL^{-3})$ - unit weight (bulk density)

$\epsilon(D)$ - linear strain

$\epsilon_r(D)$ - linear strain in the radial direction

$\epsilon_t(D)$ - linear strain in the tangential direction

$\epsilon_\theta(D)$ - linear strain in the tangential direction

$\mu(D)$ - Poisson's ratio

$\rho(L)$ - radius of curvature

$\sigma(FL^{-2})$ - normal stress

$\sigma_p(FL^{-2})$ - pillar stress P/A_p

$\bar{\sigma}_p'(D)$ - σ_p/S_o

$\sigma_p(FL^{-2})$ - average pillar stress $\Sigma P/\Sigma A_p$

$\Delta\sigma_p(FL^{-2})$ - increase in pillar stress due to mining

$\Delta\sigma_p'(D)$ - $\Delta\sigma_p/S_o$

$\sigma_r(FL^{-2})$ - radial stress

$\sigma_\theta(FL^{-2})$ - tangential stress

$\sigma_t(FL^{-2})$ - tangential stress

σ_1 (FL^{-2}) - major principal stress

σ_2 (FL^{-2}) - intermediate principal stress

σ_3 (FL^{-2}) - minor principal stress

τ (FL^{-2}) - shear stress